

Online Research @ Cardiff

This is an Open Access document downloaded from ORCA, Cardiff University's institutional repository: <https://orca.cardiff.ac.uk/id/eprint/9900/>

This is the author's version of a work that was submitted to / accepted for publication.

Citation for final published version:

Shao, Longyi, Jones, Timothy Peter ORCID: <https://orcid.org/0000-0002-4466-1260>, Gayer, Rod, Dai, Shifeng, Li, Shengsheng, Jiang, Yaofa and Zhang, Pengfei 2003. Petrology and geochemistry of the high-sulphur coals from the Upper Permian carbonate coal measures in the Heshan Coalfield, southern China. International Journal of Coal Geology 1040 , pp. 1-26. 10.1016/S0166-5162(03)00031-4 file

Publishers page: <http://www.sciencedirect.com/science/article/pii/S0166516203000314>

Please note:

Changes made as a result of publishing processes such as copy-editing, formatting and page numbers may not be reflected in this version. For the definitive version of this publication, please refer to the published source. You are advised to consult the publisher's version if you wish to cite this paper.

This version is being made available in accordance with publisher policies.

See

<http://orca.cf.ac.uk/policies.html> for usage policies. Copyright and moral rights for publications made available in ORCA are retained by the copyright holders.





Petrology and geochemistry of the high-sulphur coals from the Upper Permian carbonate coal measures in the Heshan Coalfield, southern China

Longyi Shao^{a,*}, Tim Jones^b, Rod Gayer^b, Shifeng Dai^a, Shengsheng Li^a,
Yaofa Jiang^c, Pengfei Zhang^a

^aDepartment of Resources and Earth Sciences, China University of Mining and Technology (Beijing Campus), D11 Xueyuan Road, Beijing 100083, PR China

^bDepartment of Earth Sciences, Cardiff University, P.O. Box 914, Cardiff, CF10 3YE, UK

^cJiangsu Coal Geology Research Institute, Xuzhou, Jiangsu, PR China

Received 21 August 2002; accepted 5 March 2003

Abstract

The Heshan coals, with very high organic sulphur content, are found in the Upper Permian marine carbonate successions (Heshan Formation) in the Heshan Coalfield, central Guangxi, southern China. The petrography, mineralogy, and geochemistry of coals and non-coal partings from the Suhe and Lilan coal mines of the Heshan Coalfield have been investigated using proximate, petrographic, inductively coupled plasma mass spectrometry (ICP-MS), X-ray fluorescence (XRF), X-ray diffraction (XRD), and scanning electron microscopy with an energy-dispersive X-ray (SEM-EDX) techniques. The sulphur content in the coals (with ash less than 50%) ranges from 5.3% to 11.6%, of which more than 90% is organic sulphur, reflecting a strong marine water influence on the palaeomire. The high vitrinite reflectance (1.89–2.18%Ro_{max}) indicates that the coals in the Heshan Coalfield are mainly low-volatile bituminous coal. Microscopic observation has revealed that the coal is mainly composed of vitrinite and inertinite macerals with relatively low TPI and high GI values, suggesting an unusual, strongly alkaline palaeomire, with high pH. XRD analysis plus optical and scanning electron microscopy show that the minerals in these coals are mainly quartz, calcite, dolomite, kaolinite, illite, and pyrite, although marcasite, strengite, and feldspar, as well as some oxidised weathering products such as gypsum, are also present. Most trace elements in the Heshan coals are enriched with respect to their world mean, with Mo, U, and W highly enriched, more than 10 times their world means. The trace elements are believed to be associated either with organic compounds (Mo and U) or minerals such as aluminium–iron-silicates (Sc, Ge, and Bi), aluminium-silicates (Cs, Be, Th, Pb, Ga, and REE), iron-phosphates (Zn, Rb, and Zr), iron-sulphides (As, Cd, Cr, Cu, Ni, Tl, and V), and carbonates (Sr, Mn, and W). Abnormally high organic sulphur content, high ash yields, relatively high GI values, very low TPI values, very high U contents, and very low Th/U ratios suggest that the Heshan coals accumulated in low-lying, marine-influenced palaeomires, developed on carbonate platforms. Many of these characteristics have also been recorded in the Tertiary coals of the circum-Mediterranean coal basins, where no marine

* Corresponding author. Tel./fax: +86-10-62331248x8523.

E-mail address: shaol@cumt.edu.cn (L. Shao).

influence is present. The similarities are thought to be produced by strongly alkaline groundwater chemistry, common to both environments.

© 2003 Elsevier Science B.V. All rights reserved.

Keywords: Coal; Heshan Formation; Depositional environment; Sulphur; Trace element

1. Introduction

Coal is most commonly preserved in nonmarine siliciclastic successions or paralic, interbedded siliciclastic–carbonate successions (Stach et al., 1982; Diessel, 1992). It is relatively unusual for coal to be preserved within marine carbonate successions. The Late Permian Heshan Formation in central Guangxi, southern China is composed of epicontinental marine coal-bearing carbonate successions in which mineable coal seams are directly intercalated with the marine carbonate rocks. The Heshan coal is the informal name for these coals, and they are characterised by very high organic sulphur contents and high ash yields (Shao et al., 1998). Previous studies have focused on facies and microfacies relationships and coal-forming models (Zhang et al., 1983; Zhang and Shao, 1987; Chen, 1987; Jin and Li, 1987; Shao and Zhang, 1992; Huang et al., 1994; Shao et al., 1995, 1998; Hou et al., 1995) and have demonstrated that the Heshan coals were deposited in marine carbonate platform settings. Geochemical data of this type of coal have seldom been provided. Because of their high sulphur content and therefore potential impact on the atmosphere when burnt, the coal mines producing the Heshan coals are being closed down. However, the Heshan coal will continue to be the major feed coal in some local power plants before the coal mines are fully closed.

2. Geological setting

Palaeotectonic and palaeogeographical reconstructions of the Permian in southern China have revealed that the Jiangnan basin and the Dian-Qian-Gui basin were situated between the Yangtze Block and Cathaysian Block (Wang and Jin, 2000). During the Late Permian, the current Yunnan and Guizhou Provinces occupied the western part of the Yangtze block, and

central and western Guangxi occupied most part of the Dian-Qian-Gui basin (Wang and Jin, 2000). These regions constitute a large intracratonic basin with the depositional environments ranging from nonmarine, transitional, to fully marine (Liu et al., 1993). The Late Permian siliciclastic coal measures in eastern Yunnan and western Guizhou constitute the largest coal reserves in southern China, with an overall non-marine alluvial plain and transitional paralic plain setting (China National Administration of Coal Geology, 1996). Contrasting with these areas, central Guangxi has a distinct palaeogeographic framework of isolated carbonate platforms surrounded by deep-water troughs (Sha et al., 1990; Shao and Zhang, 1992; Wang and Lu, 1994; Feng et al., 1995). The carbonate platform deposits are represented by limestones intercalated with coals (Shao et al., 1998), whereas the deep troughs are characterised by cherts with volcanoclastic turbidites (Wang and Lu, 1994) and siliciclastic submarine fan turbidites (Shao and Zhang, 1999).

The Heshan Coalfield investigated in this paper is located within one of these isolated carbonate platforms in central Guangxi. The main structure of the coalfield is an asymmetric syncline. The western limb dips 12–20°E and the steeper eastern limb dips 19–90°W, or is even overturned (Fig. 1). The coalfield is about 30 km long and 12 km wide. The Upper Permian strata in this region include the Heshan Formation and overlying Dalong Formation (Fig. 2). The base of the Upper Permian is clearly indicated by a disconformity that extends throughout most of southern China and was formed during the “Dongwu movement”, a discrete orogenic episode during the Hercynian orogeny (Han and Yang, 1980; Hu, 1994). The Permian–Triassic boundary occurs in marls in the Heshan area, and the Triassic zone fossil *Claraia wangi* is found above the inferred boundary (e.g. Liao, 1980; Shen et al., 1995). Two chronostratigraphic stages have been defined for the Late Permian

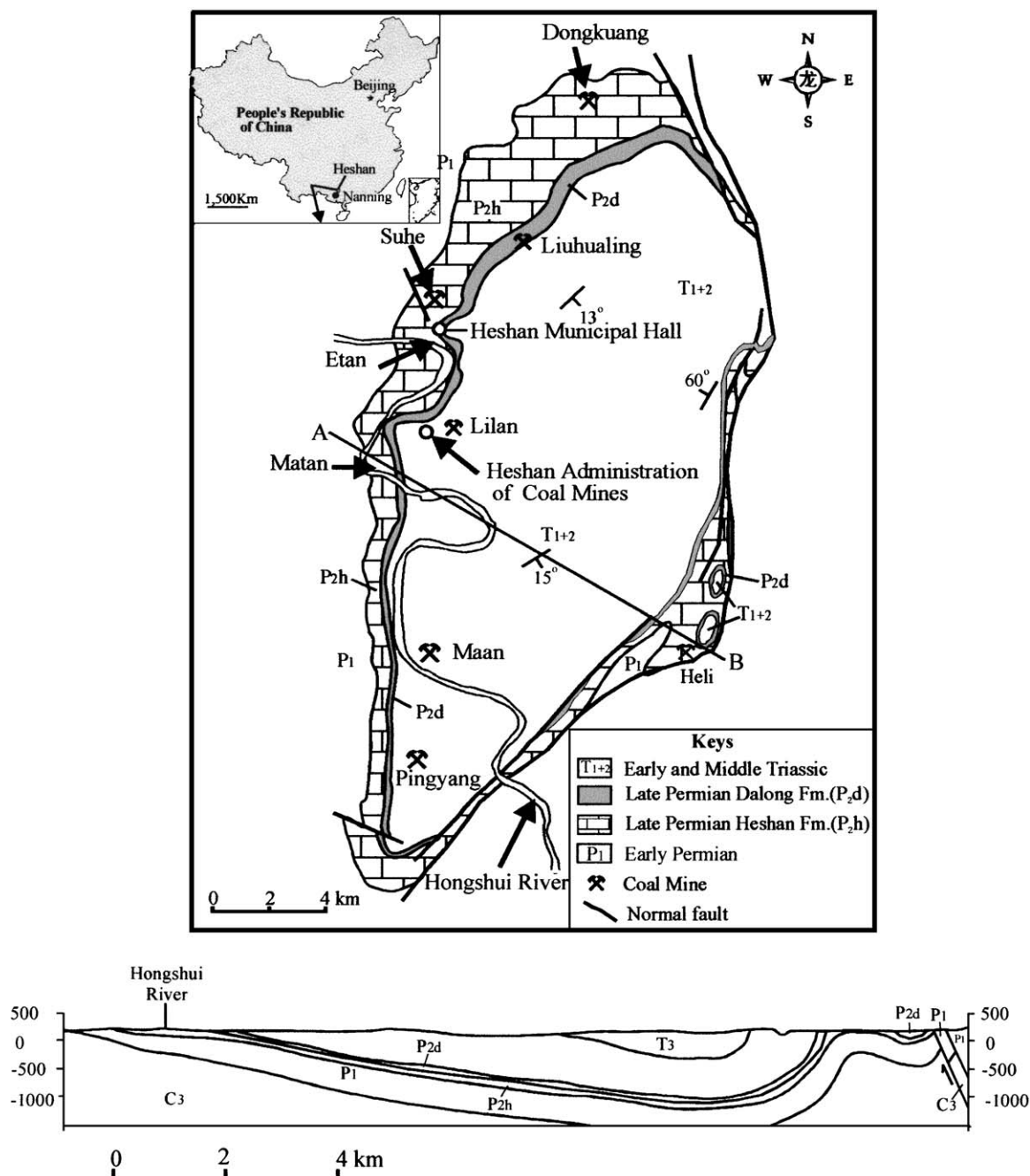


Fig. 1. Location and geological outline of the Heshan Coalfield in central Guangxi, southern China.

of this area, Wujiapingian and Changxingian (Sheng and Jin, 1994), and the boundary between these two stages is placed at the base of the limestone above

Seam 2 in the upper part of the middle Heshan Formation, based on conodont biostratigraphic data (Mei et al., 1999).

118
119
120

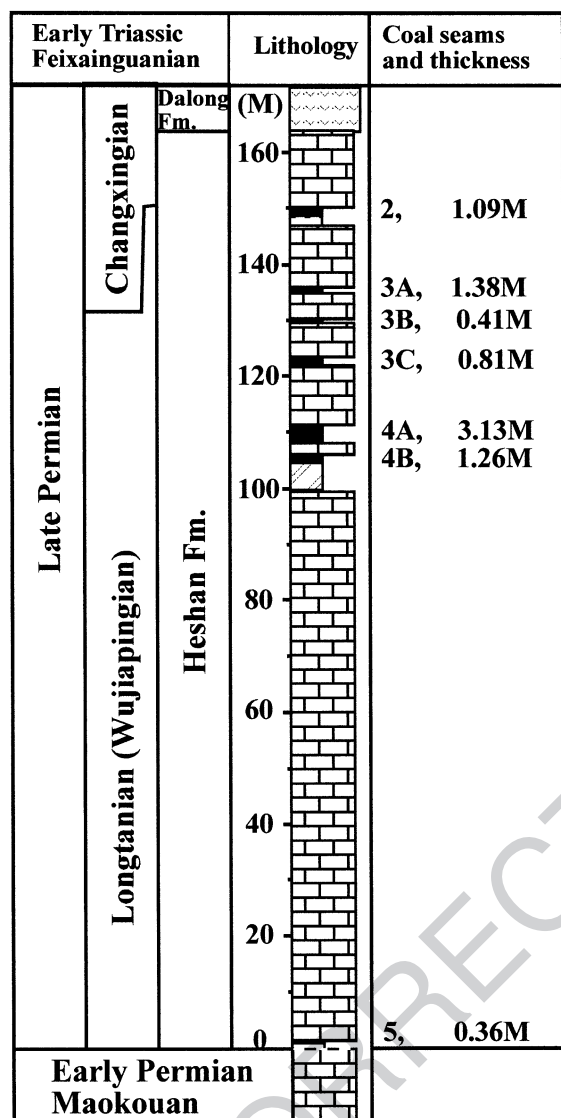


Fig. 2. Stratigraphic section of the Upper Permian coal measures in the Suhe coal mine, Heshan Coalfield.

4B, and 5, in descending order, of which Seams 3C, 4A, and 4B are major mineable seams (Fig. 2). These coal seams, together with some marker beds such as bauxitic claystones at the base of Seams 2 and 5, are widely distributed over a large area of central Guangxi, including the Heshan Coalfield (Shao et al., 1995). In particular, a discontinuity surface occurs at the base of Seam 4A, which is characterised by hummocky undulations and represents a depositional hiatus during the Late Permian (Shao and Zhang, 1992). The coals are low-volatile bituminous in rank, with the volatile matter contents ranging from 3.9% to 23.3% and a mean maximum vitrinite reflectance of 2.03% $R_{o_{max}}$. They are characterised by extremely high organic sulphur contents ranging between 6% and 10% and high ash yields ranging between 25% and 40% (Shao et al., 1998). The coal seams are usually 1 to 3 m thick, with numerous intercalations of clay. In the Lilan coal mine, coal seams 4A and 4B are amalgamated into a single seam, Seam 4. The Heshan Formation is subdivided into Lower and Upper Members, with the boundary at the base of Seam 4B, or the base of the amalgamated Seam 4.

3. Sampling and analytical methods

The coals analysed in this study are from the Suhe and Lilan underground coal mines and the Matan outcrop section, at the western side of the Heshan Coalfield (Fig. 1). Incremental channel samples were taken from the working face of both coal mines and the Matan outcrop. Both coals and interclays for each seam in the Suhe coal mine were sampled. Seam 2 is composed of carbonaceous mudstone containing marine fossils, whereas all the other seams are complicated in structure, being composed of intercalations of coals, carbonaceous mudstones, and cherts. All seams studied are within the Upper Member of the Heshan Formation, and their overall lithologies and sample numbers are shown in Fig. 3. All samples were crushed and split into quarters. One quarter was used for detailed petrographical analysis and another for geochemical analyses.

A partial proximate analysis for moisture, ash yields, and volatile matter, as well as analysis for total sulphur, were carried out on all samples, following the procedure of the British Standards Institution (BS

In the Heshan Coalfield, the Heshan Formation is about 140 m thick and consists of coal-bearing marine carbonate rocks, whereas the Dalong Formation is 20–30 m thick and is mainly composed of volcaniclastic submarine fan turbidities intercalated with thin-bedded, ammonoid-containing cherts (Shao and Zhang, 1999). There are seven recognised coal seams in the Heshan Formation, namely, 2, 3A, 3B, 3C, 4A,

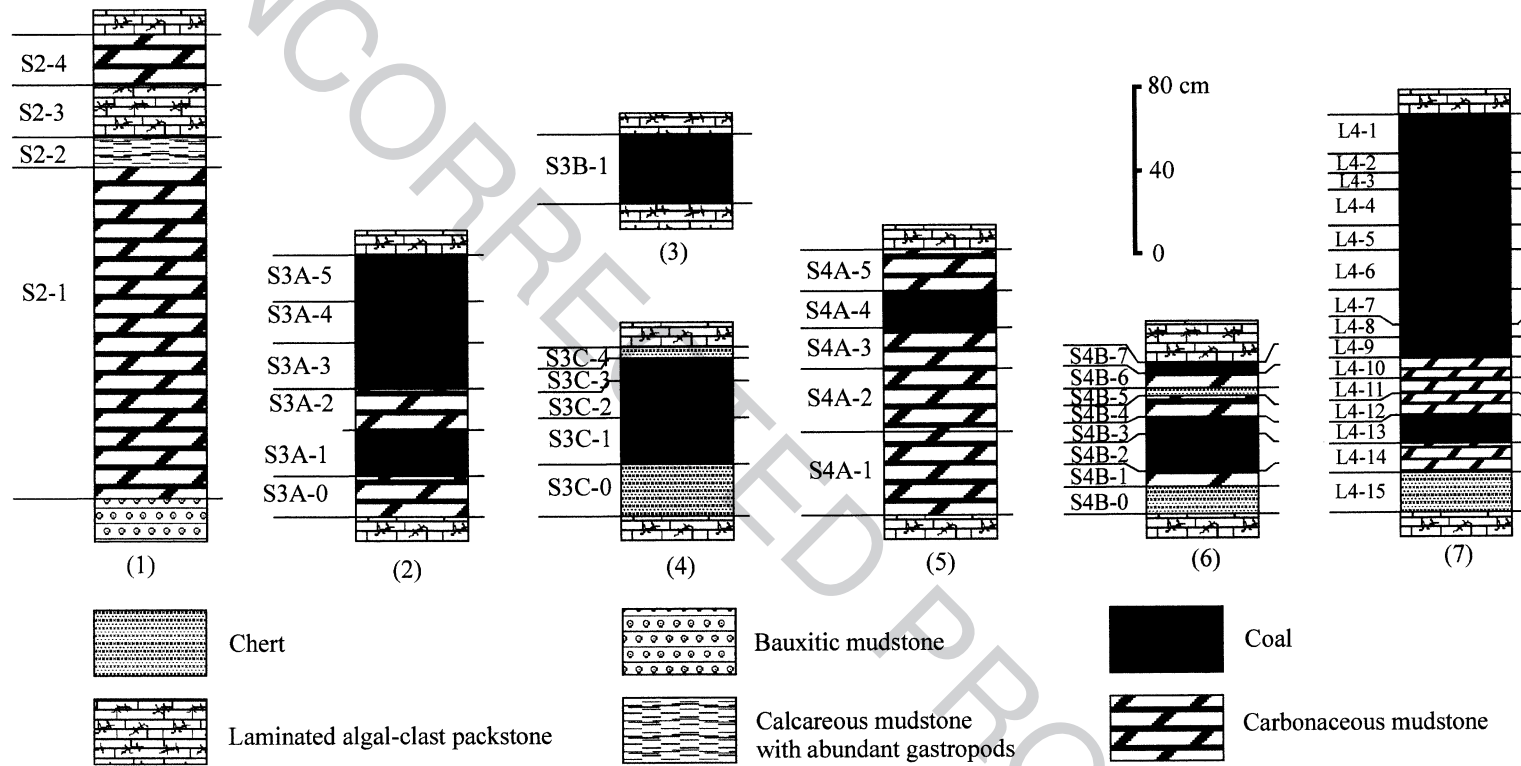


Fig. 3. Seam sections showing lithology and sample numbers of the Heshan coals in the Suhe and Lilan coal mines. (1)–(6) Suhe coal mine: (1) Seam 2, (2) Seam 3A, (3) Seam 3B, (4) Seam 3C, (5) Seam 4A, (6) Seam 4B; (7) Seam 4 in Lilan coal mine.

1016 Part 3, 1973). The total sulphur, sulphate sulphur, and pyritic sulphur of the samples from the Lilan coal mine were determined in the Jiangsu Provincial Coal Research Institute, using Beijing Coal Chemistry Institute (1982) procedures, as described by Liu et al. (2001). The petrographic characterisation of the coals was performed using standard optical reflected light microscopy. The mineral content was determined using both scanning electron microscopy with an energy-dispersive X-ray photometer (SEM-EDX) (Cambridge instruments S360 with Link AN 10000 EDX analyser) and X-ray diffraction spectrometry (XRD) (Phillips PW1710 using Cu K α radiation set at 35 kV and 40 mA with a 3–50° 2 θ range) at Cardiff University.

For the geochemical analysis, samples were ashed at 750 °C in a muffle furnace, according to the method outlined in Gayer et al. (1999). Approximately 200 mg of ash, accurately weighed, was sequentially digested, using concentrated HF, aqua regia, and 5 M HCl. A 5-ml aliquot of the diluted sample was spiked at 50 ppb with a Rh internal standard and analysed by inductively coupled plasma mass spectrometry (ICP-MS) (Perkin-Elmer Sciex Elan 5000), using an external calibration with multi-element standards. The analytical results were converted to a whole coal dry basis using the ash yield (750 °C) of each sample. It should be noted that, due to the interference of Ar–Cl with As in ICP-MS, As concentrations are likely to be slightly overestimated.

X-ray fluorescence (XRF) (Phillips PW1400, with a Cu K α source) was used to determine the major elements SiO₂, Al₂O₃, K₂O, Na₂O, Fe₂O₃, as well as the trace element Ni. Fused beads, using a flux of sodium borate, were prepared for each sample to be analysed by XRF.

SEM-EDX analysis was also used to determine the organic sulphur content of individual macerals.

4. Results and discussion

4.1. Partial proximate and ultimate analysis

Partial proximate and ultimate analysis was undertaken on the samples from the Suhe coal mine and shows that the Heshan coals have high ash yields, abnormally high sulphur contents, and relatively low-

volatile matter contents (Table 1). The ash contents, on a dry basis, are high, ranging from 13.18% to 48.93%. The higher ash contents are coincident with complex seam structures in the coals, which have a large proportion of non-coal partings of mainly carbonaceous mudstone and cherts.

The volatile matter contents of the coals (<50% ash), on a dry basis (V_{m,db}), range from 9.8% to 13.8%, with an average of 12.0%. The volatile matter content of these high ash coals is considered to be a poor indicator of rank, as a significant proportion of the volatiles is likely to have originated from minerals within the coal and ash. The vitrinite reflectance (R_{o,max}), which ranges between 1.89% and 2.18%, with an average of 2.03% (Table 4), is a more reliable rank indicator and suggests that all the seams are low-volatile bituminous coals.

The total sulphur content of the samples from the Suhe coal mine ranges between 0.37% and 11.58%, but mostly fall within 5.7% and 9.3%. These total sulphur contents show a significant inverse correlation with the ash yields (Fig. 4) and indicate that the sulphur is mainly organic sulphur. Analyses of different sulphur types have been further conducted on the coal samples from Lilan coal mine (Table 2). The total sulphur of Seam 4 from the Lilan coal mine ranges from 3.89% to 6.56%, the pyritic sulphur ranges from 0.06% to 0.25%, the sulphate sulphur ranges from <0.01% to 0.74%, and the organic sulphur ranges from 3.42% to 6.46%. It is clearly shown that the sulphur in the Heshan coals is dominated by organic sulphur that constitutes 93% of the total sulphur. The organic sulphur content of coals from the Lilan coal mine has also been estimated using energy dispersive spectroscopy of the back-scattered electrons in SEM, combined with maceral group analysis of the coals. Table 3 shows that the vitrinite group macerals have a higher organic sulphur content, ranging from 8.13% to 8.89% with an average of 8.37%, than the inertinite group macerals, which contain organic sulphur ranging from 6.85% to 7.24% with an average of 7.08%.

4.2. Petrography

Maceral analysis, using reflected light microscopy, has shown that the Heshan coals are composed of two maceral groups, consisting of 71.7–92.8% vitrinite

Table 1
Partial proximate and ultimate analysis of the Heshan coals from Suhe coal mine

Sample ID	Sample lithology	Seam	Thickness (cm)	Ash db (%)	Moisture (%)	VM db (%)	S db (%)
<i>Seam 2</i>							
2-4	carb. mudstone	top	25	79.86	2.59	20.04	1.34
2-3	algal limestone	—	25	75.03	0.44	14.90	0.37
2-2	carb. calc. mudstone	—	13	76.86	2.18	20.04	0.94
2-1	carb. mudstone	bottom	160	88.45	11.02	16.79	0.83
<i>Seam 3A</i>							
3A-5	coal	top	22	42.97	1.09	10.51	7.95
3A-4	coal	—	20	23.66	0.80	11.14	9.28
3A-3	coal	—	22	42.86	0.98	9.75	7.65
3A-2	carb. mudstone	—	20	76.99	3.50	12.43	5.73
3A-1	coal	—	22	43.73	0.81	12.49	7.74
3A-0	carb. mudstone	bottom	—	62.03	2.25	13.06	9.31
<i>Seam 3B</i>							
3B-1	coal	—	16	46.35	1.24	12.17	7.62
<i>Seam 3C</i>							
3C-4	chert	top	5	68.53	1.68	10.45	6.66
3C-3	coal	—	11	42.41	2.56	11.49	7.68
3C-2	coal	—	18	38.78	1.80	12.23	8.67
3C-1	coal	—	22	13.18	1.30	13.47	11.58
3C-0	chert	bottom	25	76.08	1.43	9.68	4.90
<i>Seam 4A</i>							
4A-5	carb. mudstone	top	20	58.50	2.45	15.28	4.13
4A-4	coal	—	18	42.60	2.40	12.86	5.34
4A-3	carb. mudstone	—	20	79.17	3.53	14.69	2.02
4A-2	carb. mudstone	—	30	75.10	4.26	14.83	4.19
4A-1	carb. mudstone	bottom	40	59.71	7.26	23.26	8.09
<i>Seam 4B</i>							
4B-7	coal	top	5	41.61	0.93	13.84	8.13
4B-6	carb. mudstone	—	7	54.32	0.70	10.55	8.32
4B-5	chert	—	4	91.17	0.45	3.94	1.02
4B-4	carb. mudstone	—	10	82.65	4.07	11.50	1.76
4B-3	coal	—	7	28.05	1.32	12.52	8.11
4B-2	coal	—	19	48.93	1.01	10.94	8.32
4B-1	carb. mudstone	—	7	63.21	1.04	9.95	6.50
4B-0	chert	bottom	13	64.60	0.93	8.75	6.11

db—dry basis; VM—volatile matter.

and 7.2–28.3% inertinite (Table 4). Liptinite group macerals have not been observed in the Heshan coals, which show no fluorescence because of their high rank (%Ro_{max} ~ 2.03). The vitrinite macerals are mainly composed of collodetrinite with some collotelinite, telinite, corpogelinite, and vitrodetrinite. Some of these vitrinite macerals may represent original liptinite group macerals that have been altered during the

coalification process, but, by comparison with related lower rank coals in which liptinite is preserved, the percentage is likely to be less than 5%. The inertinite macerals are mainly fusinite, semifusinite, and inertodetrinite, with some macrinite and micrinite.

Two maceral ratios, the gelification index (GI) and the tissue and organ preservation index (TPI), are used to reflect the degree of preservation and degradation,

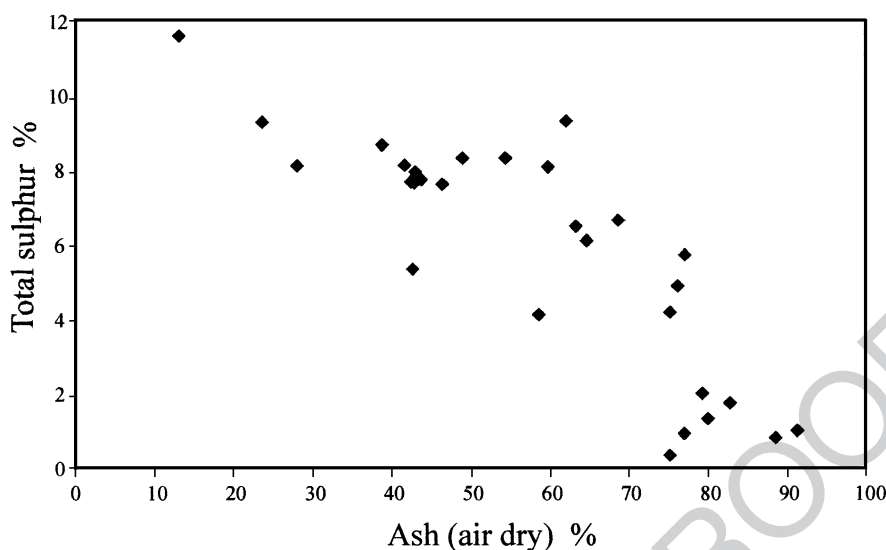


Fig. 4. Plot between the ash yields and total sulphur contents for the Heshan coals, showing a significant inverse correlation between these two components.

and to some extent, the origin of the maceral precursors (Diessel, 1986). They are defined as follows:

$$GI = \frac{(\text{Total Vitrinite} + \text{Macrinite})}{(\text{Fusinite} + \text{Semifusinite} + \text{Inertodetrinite})}$$

$$TPI = \frac{(\text{Telinite} + \text{Collotelinite} + \text{Fusinite} + \text{Semifusinite})}{(\text{Collodetrinite} + \text{Macrinite} + \text{Inertodetrinite})}$$

Conditions of relatively high water level are indicated by GI values greater than 2.0, whereas GI values

less than 2.0 indicate relatively low water levels. TPI values higher than 1 indicate wet conditions, whereas TPI values lower than 1 indicate dry conditions. In addition to these interpretations, Gentzis and Goodarzi (1990) suggested that the GI and TPI values can provide information on the chemistry of the coal-forming environment, such as redox-potential and pH values. Acidic conditions inhibit bacterial activity and decay of plant material, resulting in a relatively high abundance of well-preserved plant structures and high values of TPI. Alkaline conditions permit bacterial activity and decay of plant material, resulting in relatively low preservation of plant structure and low values of TPI.

GI and TPI values have been calculated for the Heshan coal and results are given in Table 4. All these

Table 2

Sulphur in Seam 4, the Lilan coal mine

Sample ID	St, ad (%)	Sp, d (%)	Ss, d (%)	So, d (%)
L4-1	3.89	0.25	0.22	3.42
L4-3	5.52	0.1	0.1	5.32
L4-4	6.08	0.06	0.01	6.01
L4-6	6.2	0.14	0	6.06
L4-8	6.56	0.08	0.2	6.28
L4-12	4.96	0.24	0.5	4.22
L4-14	5.64	0.18	0.74	4.72
Min.	3.89	0.06	0.00	3.42
Max.	6.56	0.25	0.74	6.28
Mean	5.55	0.15	0.25	5.15
S.D.	0.90	0.08	0.27	1.07

Table 3

Organic sulphur detected by SEM-EDX for coals of Seam 4 in the Lilan coal mine

		Vitrinite					Inertinite				
	Points	Min.	Max.	Mean	S.D.	Points	Min.	Max.	Mean	S.D.	
L4-1	1	8.17	8.17	8.17	3	7.08	7.19	7.12	0.06		
L4-2	12	7.08	9.43	8.44	0.84	6	6.67	7.45	7.03	0.29	
L4-4	5	7.28	8.70	8.13	0.63	4	6.98	7.36	7.24	0.18	
L4-5	4	7.98	8.40	8.23	0.18	5	6.08	7.37	6.85	0.52	
L4-7	5	8.64	9.06	8.89	0.17	6	6.72	7.47	7.19	0.28	

t4.1 Table 4

t4.2 Maceral and mineral contents and vitrinite reflectance of the Heshan coals from the Suhe coal mine

t4.5	Sample ID	Maceral components as percentage of total maceral content													Mineral components (vol.%)					V/I	GI	TPI	Vitrinite reflectance		
		Total maceral vol.%	Vitrinite macerals						Inertinite macerals						M _{total}	Py	Q	Carb	Clay				Ro _{max} %	Ro _{min} %	Ro _{rand} %
			V _{total}	T	CT	CD	CG	VD	I _{total}	MIC	MAC	SF	F	ID											
t4.6	3A-5	65.2	81.7	8.3	8.7	58.7	0.6	5.4	18.3	0.0	0.6	3.1	3.5	11.0	34.8	2.5	1.0	0.6	30.7	4.5	4.67	0.34			
t4.7	3A-4	66.5	77.4	0.0	3.0	57.7	0.0	16.7	22.4	0.5	1.7	3.5	7.1	9.8	33.5	2.4	1.3	1.1	28.7	3.5	3.90	0.20	1.96	1.83	1.9
t4.8	3A-3	64.8	81.8	2.2	10.2	62.2	0.9	6.3	18.2	0.0	1.4	1.9	5.2	9.7	35.2	0.9		0.8	33.5	4.5	4.94	0.27			
t4.9	3A-1	77.2	83.5	0.9	8.8	65.0	0.0	8.8	16.6	0.0	4.7	5.1	6.0	0.9	22.8	5.7	6.4	1.8	8.9	5.0	7.40	0.29	1.98	1.7	1.85
t4.10	3B-1	56.2	74.7	2.0	8.2	48.6	4.1	11.9	25.3	0.5	3.2	0.0	7.5	14.1	43.8	3.1	1.5	0.7	38.5	3.0	3.62	0.27			
t4.11	3C-3	59.2	80.7	2.1	2.7	68.4	0.0	7.6	19.6	0.3	0.7	2.0	2.4	14.2	40.8	1.2	0.8	0.4	38.4	4.1	4.38	0.11			
t4.12	3C-2	48.1	71.7	5.4	2.3	17.0	1.5	45.5	28.3	0.0	0.0	5.4	3.1	19.8	51.9	9.7	3.8	0.4	38.0	2.5	2.54	0.44	2.07	1.85	1.96
t4.13	3C-1	77.2	89.9	4.7	3.2	72.2	1.0	8.8	10.2	1.0	0.0	2.2	1.2	5.8	22.8	1.9	1.1	0.6	19.2	8.8	9.77	0.14	2.18	1.95	2.04
t4.14	4A-4	58.6	69.5	7.0	4.1	22.5	3.8	32.1	30.5	1.7	0.0	7.8	5.5	15.5	41.4	3.0	1.9	1.0	35.5	2.3	2.41	0.64	2.06	1.84	1.95
t4.15	4B-7	68.7	86.0	1.3	9.2	67.8	0.6	7.1	14.3	0.0	0.6	4.5	7.9	1.3	31.3	3.1	1.8	16.1	10.3	6.0	6.33	0.33	1.89	1.69	1.8
t4.16	4B-3	76.3	92.8	0.8	2.9	87.8	0.0	1.3	7.2	0.0	1.3	3.8	1.7	0.4	23.7	2.5	6.0	0.6	14.6	12.9	15.96	0.10			
t4.17	4B-2	71.9	76.4	5.0	13.8	41.3	0.4	15.9	23.6	2.8	2.8	7.8	6.4	3.9	28.1	9.1	1.5	2.8	14.7	3.2	4.38	0.69	2.06	1.85	1.96

V—vitrinite; CD—collodetrinite; CT—collotelinite; T—telinite; CG—corpogelinite; VD—vitrodetrinite; I—inertinite; F—fusinite; SF—semifusinite; MIC—micrinite; MAC—macrinite; ID—inertodetrinite; Q—quartz; PY—pyrite; Carb—carbonate; Ro—Vitrinite reflectance in oil; Ro_{max}—the mean maximum reflectance of vitrinites; Ro_{min}—the mean minimum reflectance of vitrinites; Ro_{rand}—the mean random reflectance of vitrinites; GI—gelification index=(Total Vitrinite + Macrinite)/(Fusinite + Semifusinite + Inertodetrinite);

t4.18 TPI—tissue preservation index=(Telinite + Collotelinite + Fusinite + Semifusinite)/(Collodetrinite + Macrinite + Inertodetrinite).

306 coals have GI values between 2.41 and 15.96, and TPI
 307 values between 0.10 and 0.69. As discussed above,
 308 some of the vitrinite macerals may have been derived
 309 from liptinite macerals during coalification. This is
 310 thought to account for less than 5% of the total
 311 vitrinite and has resulted in slightly raised GI values
 312 (by less than 0.3%) and probably very slightly raised
 313 TPI values. Nevertheless, because these maceral indi-
 314 ces were established for lower rank coals (Diessel,
 315 1982), there remains some uncertainty in their use
 316 with low-volatile bituminous coals. The GI values of
 317 the Heshan coals are relatively high, similar to some
 318 other marine transgressive coals such as the Wynn
 319 Seam of the Permian in New South Wales (Diessel,
 320 1992) and the Amman Rider seam of the Pennsylvanian
 321 in South Wales (Gayer et al., 1999). However,
 322 the TPI values are generally lower than these marine
 323 transgressive coals. These relatively high GI values
 324 and very low TPI values suggest high levels of
 325 microbial activity and relatively deep, alkaline water

326 conditions. This is consistent with an overall marine
 327 carbonate platform setting. The variations of the GI
 328 and TPI values (Fig. 5) indicate that the peat mire
 329 experienced episodic changes in its hydrology. Regular
 330 flooding of the peat surface introduced oxygenated
 331 waters and nutrients into the peat, thus promoting
 332 microbial degradation and oxidation of the organic
 333 matter (Stach et al., 1982).

4.3. Mineralogy and major element geochemistry

336 The ash yields are generally high in the Heshan
 337 coals due to the complex seam structures and mud-
 338 stone partings in the coals. There are also a large
 339 variety of minerals in the coals. Microscopic obser-
 340 vation has revealed that the mineral component is
 341 normally higher than 30% by volume, ranging
 342 between 22.8% and 51.9%. These comprise clay
 343 minerals (8.9–38.5%), pyrite (0.9–9.7%), quartz
 344 (0.8–6.4%), and carbonates (0.4–16.1%). Table 5

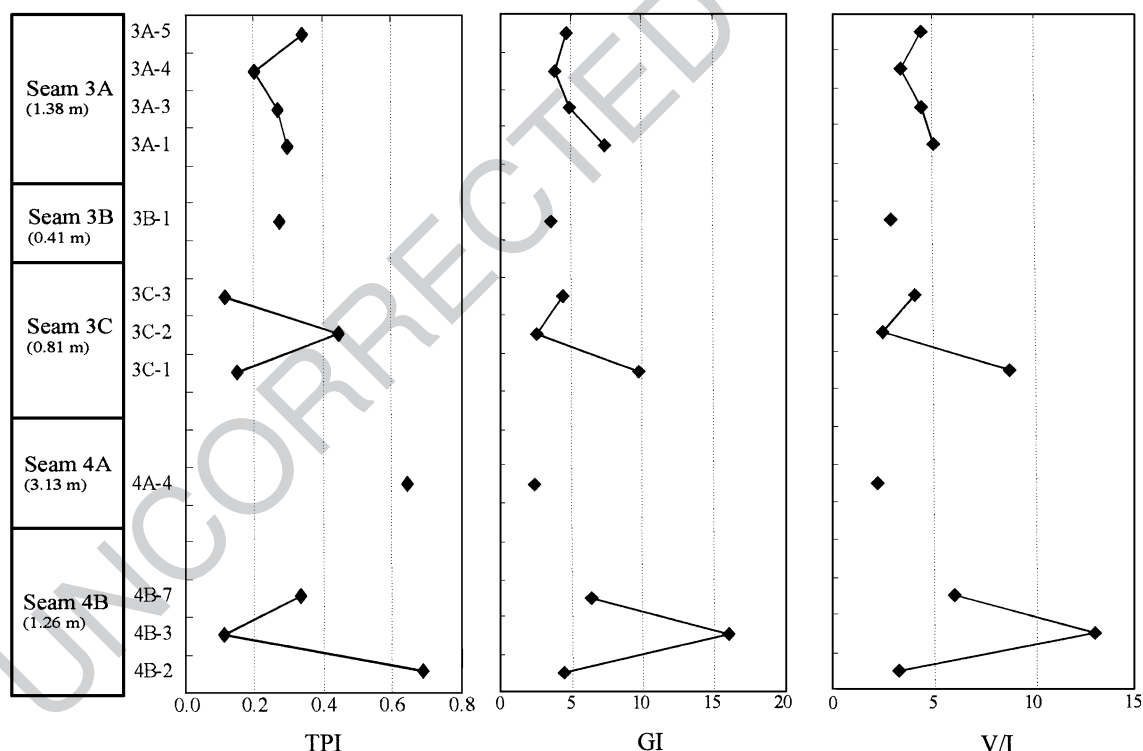


Fig. 5. Vertical trends for some petrographic characteristics of the Heshan coals in the Suhe coal mine of the Heshan coalfield. V/I= ratio of vitrinite and intertinite; GI= gelification index; TPI= tissue preservation index (for explanation, see text and Table 4). No vertical scale is intended but the thickness of each coal seam is given following the name of the seam number.

Table 5

Semiquantitative data of mineral compositions in the Heshan coals inferred by the XRD analyses and recalculated with ash contents (in %)

	Seams	Illite	Kaolinite	Quartz	Pyrite	Marcasite	Calcite	Dolomite	Strengite	Anatase	Gypsum	Albite
t5.4	2-4	2.6	1.4	28.3	2.1		43.3		2.2			
t5.5	2-3			14.1	0.7		60.3					
t5.6	2-2	1.5		21.6	0.8		52.9					
t5.7	2-1	15.1	5.6	52.3	4.0		0.7		0.6	9.6		0.6
t5.8	3A-5	2.3		37.6	0.9		1.7	0.4				
t5.9	3A-4	1.2		18.0	0.6		0.9	0.7	0.2	1.4		0.6
t5.10	3A-3		0.9	38.7	0.4		0.6	1.9		0.3		
t5.11	3A-2	15.0	0.9	39.1	5.7		1.4	13.1	0.9			1.0
t5.12	3A-1	2.2		30.8	2.1	0.1	3.5	4.6	0.2	0.1		
t5.13	3A-0	1.6	2.4	47.2	6.7	0.9			2.9	0.4		
t5.14	3B-1	1.6	0.9	38.4	2.3		0.5	2.3	0.3			
t5.15	3C-4	2.4		60.8	2.3		3.0					
t5.16	3C-3	2.0	0.8	38.4			0.4	0.7				
t5.17	3C-2	3.1		32.0	1.3	0.5	0.8	0.7	0.3			
t5.18	3C-1		3.0	4.3	1.7	1.2			0.3	2.2	0.6	
t5.19	3C-0	1.4		71.5	1.1				1.5			0.5
t5.20	4A-5	2.0	40.5	6.0	2.5		2.5	2.5		2.3	0.3	
t5.21	4A-4	1.1	25.2	10.7		1.8	1.2	1.0		1.0	0.6	
t5.22	4A-3	5.0	33.5	26.9	2.2	0.4	5.9	1.0		1.3	3.1	
t5.23	4A-2	8.3	21.3	31.7	3.2	0.4		1.1	7.3	0.7	1.1	
t5.24	4A-1	14.0	1.6	21.8	8.5	1.0	1.6	2.4	2.0	4.3	2.5	
t5.25	4B-7	1.8	3.1	26.1	3.2		4.6	1.9	0.5	0.3		
t5.26	4B-6	1.0	3.1	44.0	4.2				1.8	0.2		
t5.27	4B-5		1.8	72.9	2.7		9.0	4.7				
t5.28	4B-4	20.7		57.0			0.4	0.9	0.2	2.8		0.6
t5.29	4B-3	12.8		11.7	0.7		0.8	1.0	0.3	0.7		
t5.30	4B-2	5.1		37.9	2.5	0.6		1.1	0.9	0.7		
t5.31	4B-1	0.8	0.3	55.4	2.2			2.2	1.9	0.4		
t5.32	4B-0	3.2		57.5	2.7				1.3			

summarises the semiquantitative results of the mineralogical composition of the Heshan coals determined from the XRD analysis. Quartz, calcite, dolomite, kaolinite, illite, and pyrite are the most abundant minerals (Fig. 6). Marcasite, mixed-layer clays, strengite, anatase, and feldspar, as well as some weathering oxidation products such as gypsum and haematite, are also present. The clay minerals kaolinite and illite normally occur admixed with the coal material except in a few instances, where they form alteration products replacing euhedral calcite and dolomite. Pyrite is mainly either syngenetic or early epigenetic in origin, occurring as framboidal, euhedral, and subhedral crystals within the coal (Fig. 7). Euhedral quartz crystals occur enveloped by coal laminae (Fig. 7), implying a pre-coal compaction origin probably resulting from subaerial volcanism during coal accumulation. Carbonates are common in some coals. Dolomite crystals are also enveloped by

coal laminae (Fig. 7), indicating early dolomitisation before peat compaction (Shao et al., 1998).

Table 6 lists the major and trace element compositions of the Heshan coals. In general, elements in coal occur either associated with the inorganic constituents (minerals) or with organic constituents (Finkelman and Gross, 1999; Spears and Zheng, 1999; Querol et al., 1999; Gayer et al., 1999; Karayigit et al., 2001; Zhuang et al., 2000). The mode of occurrence of an element in coal can be inferred from its association with particular minerals or major elements, based on the Pearson's correlation coefficients between elements. Elements with positive correlations with the ash yields indicate an inorganic association suggesting that the elements are combined in minerals in the coal. Elements that do not correlate with the ash yields may either have an organic association or a mixed mode of occurrence in the coal. Nicholls (1968) suggested that elements that were organically bound in a coal would show a neg-

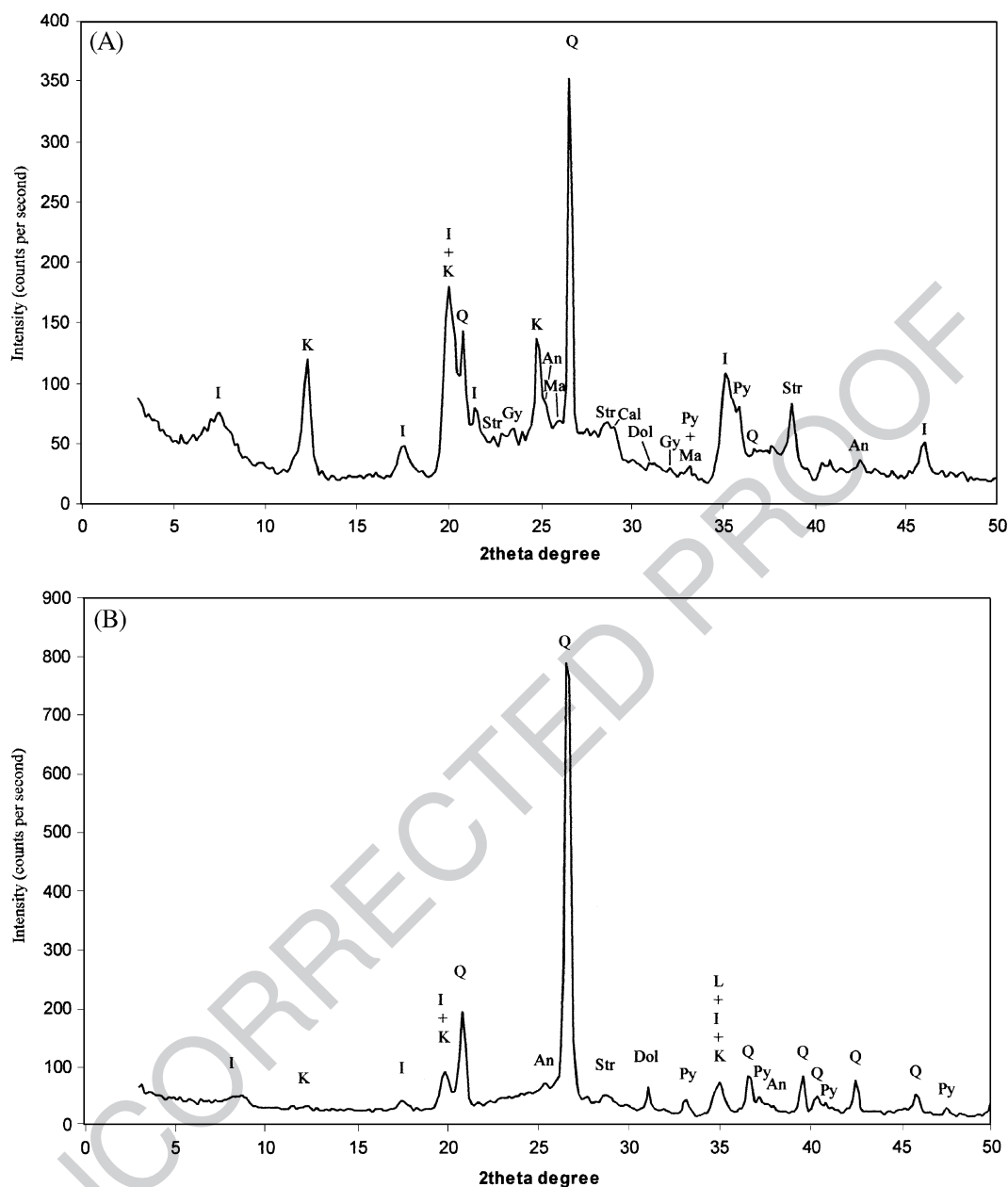


Fig. 6. XRD spectra for the Heshan Coals from the Suhe coal mine in the Heshan Coalfield. (A) Seam 4A-2; (B) Seam 4B-1. An—anatase; Cal—calcite; Dol—dolomite; Gy—gypsum; I—illite; K—kaolinite; Ma—marcasite; Py—pyrite; Q—quartz; Str—strengite.

active linear or curvilinear relationship with the ash yield when plotted as a concentration in the ash. This is because the increasing ash content dilutes the concentration of the element in the ash. However, the effect cannot normally be detected above an ash yield of

about 25%. These relationships can usually be inferred by the Pearson's correlation coefficients between pairs of elements or between element and ash yield. In the Heshan Formation, four chert samples (3C-4, 3C-0, 4B-5, and 4B-0) with very high SiO_2 contents have

388
389
390
391
392

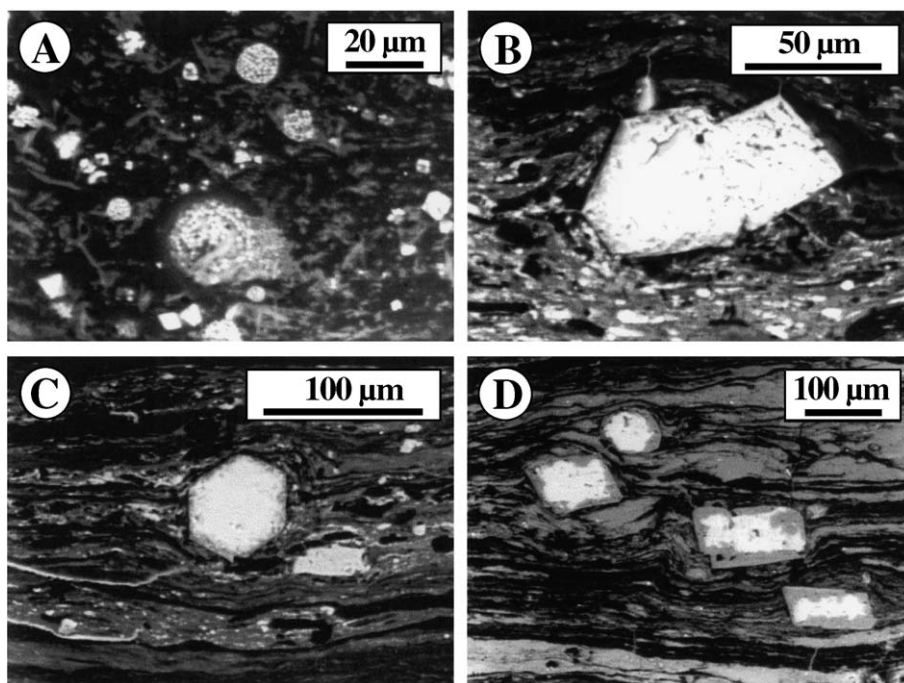


Fig. 7. SEM four-quadrant backscatter images of polished blocks showing some minerals in Seam 4 from the Lilan coal mine, Heshan Coalfield, central Guangxi. (A) Framboidal, euhedral and subhedral pyrite crystals; (B) euhedral hexagonal quartz crystal (left) and compositionally zoned dolomite crystal with rims (right); (C) euhedral hexagonal quartz crystal; (D) calcite crystals. All these crystals are enveloped by vitrinite laminae, indicating a pre-compaction, syngenetic origin for these minerals.

393 been excluded from our Pearson's correlation analysis.
 394 In the Heshan coals, most major elements show positive
 395 correlation with the ash yields at the 95% confidence level;
 396 they are SiO_2 ($r=0.52$), Al_2O_3 ($r=0.58$), CaO ($r=0.4$),
 397 MgO (0.36), Na_2O ($r=0.73$), TiO_2 ($r=0.57$), and
 398 P_2O_5 ($r=0.44$), indicating that these elements are mainly
 399 associated with minerals. K_2O and Fe show no correlation
 400 with the ash yields, and this is due to the influence of
 401 calcareous and carbonate rocks in the upper part of Seam 2.
 402 If we exclude three samples from that seam which have more
 403 than 10% of CaO , the correlation of K_2O and Fe with the
 404 ash yields become significant, with the coefficients being 0.33
 405 and 0.39, respectively. This suggests that K and Fe in the
 406 coals are also mainly associated with minerals.

408 Abundant Al_2O_3 in the Heshan coals demonstrates
 409 the dominance of detrital clay minerals in the coals, which
 410 is consistent with the occurrence of illite, kaolinite, and
 411 illite/smectite mixed layers identified by the XRD analysis.
 412 Although SiO_2 and Al_2O_3 are positively correlated with
 413 the ash yields, they do not

show a significant intercorrelation ($r=0.30$), suggesting
 that SiO_2 has another source in addition to clay minerals.
 The abundant quartz identified by the XRD analysis suggests
 that the extra SiO_2 is present in the form of quartz. The
 highest level of SiO_2 occurs in the cherty bands in the 4B
 and 3C coal seams.

CaO in the Heshan coals ranges between 0.22% and
 37.12%, with an average of 4.32%, and is present in the
 form of carbonate minerals. High levels of calcite and
 dolomite were identified by the XRD analysis. Na_2O is
 positively correlated with CaO , with a coefficient of 0.66,
 suggesting that Na is mainly associated with carbonate
 minerals, which is a surprising result, as Na is normally
 associated with silicates (e.g. Querol et al., 1998).

The MgO contents in the Heshan coals are between 0.27%
 and 2.18%, with an average of 0.85%, and show strong
 association with SiO_2 as well as with K_2O . As K is most
 commonly found in illites, these associations may suggest
 that the K, Si, and Mg are present in the clay minerals,
 illite, or illite/smectite

Table 6

Major and trace elements of the Heshan coals from the Suhe coal mine

t6.3	Sample no.	2-4	2-3	2-2	2-1	3A-5	3A-4	3A-3	3A-2	3A-1	3A-0	3B-1	3C-4	3C-3	3C-2
t6.4	in %														
t6.5	Ash	79.86	75.03	76.86	88.45	42.97	23.66	42.86	76.99	43.73	62.03	46.35	68.53	42.41	38.78
t6.6	St	1.34	0.37	0.94	0.83	7.95	9.28	7.65	5.73	7.74	9.31	7.62	6.66	7.68	8.67
t6.7	SiO ₂	27.44	15.90	21.65	19.55	19.83	16.84	26.94	31.17	21.76	31.98	24.07	37.73	22.47	20.66
t6.8	Al ₂ O ₃	9.52	2.58	6.51	9.37	4.12	3.90	3.56	13.42	4.75	7.75	5.14	5.89	4.52	4.83
t6.9	CaO	19.69	37.12	26.53	1.42	0.75	0.42	1.17	2.29	3.12	0.38	1.12	0.29	0.53	0.59
t6.10	MgO	0.48	0.78	1.08	0.73	0.56	0.36	0.90	1.74	1.70	0.93	1.03	0.86	0.68	0.71
t6.11	K ₂ O	0.73	0.11	0.50	0.91	0.79	0.76	0.32	1.57	0.80	0.51	0.45	0.62	0.58	0.77
t6.12	Na ₂ O	0.33	0.44	0.39	0.28	<0.01	<0.01	<0.01	0.08	<0.01	<0.01	<0.01	0.02	<0.01	<0.01
t6.13	Fe	1.01	0.37	0.96	3.22	0.60	0.30	0.44	1.21	0.84	2.78	1.35	1.60	0.74	1.13
t6.14	TiO ₂	0.31	0.11	0.25	0.74	0.15	0.15	0.14	0.45	0.21	0.31	0.37	0.53	0.23	0.23
t6.15	P ₂ O ₅	0.006	0.013	0.007	0.024	0.004	0.005	0.007	0.012	0.007	0.016	0.009	0.007	0.010	0.009
t6.16	in ppm														
t6.18	As	20.7	12.4	19.9	36.0	15.7	2.1	3.6	15.6	4.5	20.5	11.2	6.7	7.5	9.6
t6.19	Ba	36.2	27.4	27.7	53.3	51.6	53.3	321.9	106.5	83.4	54.5	33.8	56.8	143.8	104.0
t6.20	Be	1.4	0.3	1.0	3.4	1.4	4.1	1.7	4.1	3.6	1.8	1.1	0.6	0.9	1.2
t6.21	Bi	0.6	0.2	0.4	1.2	0.3	0.2	0.1	0.6	0.4	1.1	0.4	0.3	0.6	0.3
t6.22	Cd	0.2	0.0	0.1	0.0	0.9	0.3	0.5	0.7	0.5	0.8	1.2	0.2	0.2	0.2
t6.23	Co	9.9	9.8	14.8	7.4	3.9	15.9	6.3	10.9	9.5	11.8	8.1	11.8	17.1	8.5
t6.24	Cr	58.3	27.4	42.7	88.0	35.8	12.7	12.3	12.4	30.0	43.3	104.8	6.7	11.2	12.7
t6.25	Cs	3.9	0.5	2.5	9.8	3.0	2.5	2.1	11.1	3.7	4.9	4.8	6.1	5.5	5.9
t6.26	Cu	7.3	4.3	5.4	10.4	9.9	8.2	10.6	26.3	14.3	17.3	23.1	13.7	4.5	9.8
t6.27	Ga	14.4	3.4	9.7	28.2	8.1	9.7	7.3	26.1	10.4	9.0	7.8	7.5	7.2	7.8
t6.28	Ge	0.9	0.4	0.6	1.4	0.3	0.5	0.4	0.4	0.5	0.5	0.3	0.3	0.3	0.4
t6.29	Mn	151.1	221.3	169.0	79.6	65.5	14.7	34.1	166.1	46.1	134.4	128.7	192.3	54.9	114.3
t6.30	Mo	13.5	7.7	13.5	13.3	111.2	24.8	23.5	22.6	134.2	132.5	119.7	9.6	17.4	26.9
t6.31	Nb	10.0	4.2	8.1	20.9	9.9	17.0	16.2	10.2	8.3	26.8	13.3	2.8	7.2	7.1
t6.32	Ni	<1	<1	<1	<1	10	<1	<1	<1	9	4	27	<1	<1	<1
t6.33	Pb	24.4	9.0	22.3	45.5	16.3	8.9	38.1	43.9	11.4	30.8	11.7	10.9	17.1	15.6
t6.34	Rb	39.9	5.4	26.3	83.5	42.7	33.4	21.0	84.8	38.6	33.1	25.9	29.9	28.8	34.1
t6.35	Sc	7.3	3.4	7.2	17.5	5.7	8.7	4.9	13.5	8.0	9.1	6.6	5.5	5.3	5.8
t6.36	Sr	1688.7	3388.7	3147.4	311.5	151.7	200.4	226.7	379.3	345.6	202.3	230.3	344.4	878.8	1465.0
t6.37	Ta	1.8	2.2	2.4	2.9	0.7	0.6	0.6	1.3	1.0	1.8	0.9	0.7	1.2	0.9
t6.38	Th	20.4	3.6	14.0	43.3	12.9	9.6	33.3	17.4	9.1	58.5	16.6	5.9	7.8	9.5
t6.39	Tl	0.3	0.1	0.1	0.3	1.5	0.8	1.7	2.0	1.8	4.2	2.2	0.3	0.9	1.0
t6.40	U	8.7	7.0	6.9	13.0	125.5	44.0	41.0	37.9	175.8	87.3	117.6	9.2	21.1	37.0
t6.41	V	137.7	65.4	124.5	188.7	197.4	48.7	40.0	44.9	239.0	247.4	273.5	35.1	31.1	45.3
t6.42	W	75.1	130.2	84.3	14.7	26.3	53.1	64.0	27.0	42.1	56.8	36.6	42.1	71.6	44.6
t6.43	Y	13.5	26.8	21.9	30.8	17.2	91.3	53.9	37.1	92.3	78.4	27.7	7.8	14.2	13.6
t6.44	Zn	32.6	13.4	32.5	61.2	58.1	38.5	98.5	71.6	43.5	63.9	64.2	35.6	28.7	40.7
t6.45	Zr	142.5	47.1	103.6	815.8	174.9	144.3	152.0	195.9	135.9	746.5	211.7	72.4	84.9	76.5
t6.46	La	28.2	21.8	27.3	45.4	7.9	34.4	42.3	25.7	50.5	34.2	7.7	5.0	13.7	12.7
t6.47	Ce	72.3	38.9	70.9	95.3	18.5	85.0	89.6	61.6	115.8	75.6	23.9	12.0	30.5	30.0
t6.48	Pr	8.4	4.5	8.7	8.7	2.4	11.7	11.1	7.9	16.0	9.3	3.5	1.6	3.9	3.6
t6.49	Nd	32.6	16.3	34.0	28.9	9.3	46.6	42.1	31.9	67.2	35.2	14.1	6.0	13.9	14.2
t6.50	Sm	7.1	4.2	8.1	6.2	2.6	13.0	9.8	7.8	17.4	9.6	4.5	1.5	2.9	3.2
t6.51	Eu	1.0	0.9	1.5	1.0	0.5	1.7	1.2	1.3	2.5	1.5	0.9	0.4	0.7	0.7
t6.52	Gd	5.9	5.4	8.1	6.7	3.0	15.6	10.7	8.0	19.8	11.5	5.1	1.5	3.2	3.4
t6.53	Tb	0.9	0.9	1.3	1.2	0.6	3.0	1.9	1.3	3.3	2.6	1.1	0.3	0.6	0.6
t6.54	Dy	4.7	6.2	6.5	7.9	4.0	20.2	11.8	8.0	19.8	17.5	7.4	2.1	3.9	3.4
t6.55	Ho	0.8	1.3	1.1	1.7	0.9	4.2	2.4	1.6	4.2	3.9	1.7	0.4	0.8	0.7
t6.56	Er	2.3	3.7	2.9	4.8	2.8	12.8	7.5	4.6	11.8	12.3	5.3	1.4	2.3	2.0

3C-1	3C-0	4A-5	4A-4	4A-3	4A-2	4A-1	4B-7	4B-6	4B-5	4B-4	4B-3	4B-2	4B-1	4B-0
13.18	76.08	58.50	42.60	79.17	75.10	59.71	41.61	54.32	91.17	82.65	28.05	48.93	63.21	64.60
11.58	4.90	4.13	5.34	2.02	4.19	8.09	8.13	8.32	1.02	1.76	8.11	8.32	6.50	6.11
7.26	35.75	21.69	19.35	24.04	23.30	21.86	15.25	30.14	42.06	28.96	15.35	26.52	35.79	35.38
2.58	4.31	15.92	12.17	16.23	15.78	11.11	4.89	3.76	2.88	12.71	6.87	7.35	7.29	6.38
0.61	0.26	2.47	0.53	2.38	0.28	0.31	3.83	0.48	1.04	0.84	0.22	0.29	0.74	0.16
0.27	0.52	0.28	0.32	0.51	0.44	1.11	0.75	0.70	0.42	2.18	0.63	0.99	1.44	0.99
0.51	0.68	0.23	0.37	0.41	0.49	1.28	0.62	0.73	0.22	1.11	0.63	1.15	1.16	1.09
<0.01	0.08	0.08	0.04	0.31	0.48	0.02	<0.01	<0.01	0.10	0.17	<0.1	<0.1	<0.1	<0.1
0.81	1.34	0.65	0.44	0.50	1.09	3.12	1.03	2.05	0.27	<0.1	0.02	1.40	1.44	1.39
0.13	0.32	0.47	0.39	0.59	0.65	0.59	0.33	0.48	0.16	1.01	0.49	0.35	0.42	0.42
0.004	0.021	0.003	0.004	0.005	0.008	0.010	0.006	0.009	0.004	0.004	0.004	0.005	0.007	0.008
3.3	7.3	2.4	2.1	2.4	11.8	24.8	54.9	70.1	12.4	8.1	6.8	41.7	61.2	62.0
34.1	51.4	49.3	63.6	74.3	86.7	151.6	56.6	73.0	62.3	68.9	60.5	87.8	109.7	112.4
1.5	0.4	2.6	2.0	4.4	4.0	6.5	2.1	1.8	0.6	4.7	3.6	2.7	3.3	3.1
0.4	0.3	1.1	0.8	1.7	2.6	1.5	0.6	1.0	0.3	1.0	0.6	0.8	1.0	1.0
0.4	0.2	0.2	0.0	0.3	0.2	3.2	1.2	1.2	0.4	0.2	0.3	0.2	0.5	0.5
6.2	13.0	8.1	3.4	6.0	23.0	17.2	3.6	11.4	11.4	5.6	3.8	19.9	8.7	7.7
17.2	6.2	12.9	25.1	53.2	74.1	321.3	157.5	242.0	45.9	5.3	38.5	227.3	238.8	246.9
1.8	3.3	3.0	5.0	7.2	7.4	18.0	4.4	6.0	1.8	17.6	12.5	10.0	9.5	9.6
7.5	8.9	20.0	12.1	9.4	12.1	30.2	11.4	16.6	5.5	6.4	15.0	16.1	13.9	15.4
7.9	4.0	25.0	23.1	33.9	32.4	23.1	13.0	16.3	5.4	28.4	18.7	11.8	12.0	12.5
0.5	0.2	0.8	0.7	1.3	1.7	1.0	0.6	0.8	0.4	0.6	0.5	0.4	0.6	0.6
24.7	270.9	7.6	4.0	11.3	19.7	77.8	79.6	56.1	21.1	18.6	9.1	37.4	84.8	82.2
72.1	4.0	10.2	4.5	2.5	15.8	50.3	171.7	136.7	13.1	14.8	15.7	71.9	33.6	35.3
11.3	3.1	19.2	14.7	24.3	27.6	28.7	117.5	35.3	9.0	119.2	30.2	28.0	22.1	22.6
<1	<1	<1	<1	<1	<1	22	21	26	<1	<1	<1	22	16	15
9.0	9.9	48.5	39.4	49.1	135.3	49.8	20.5	29.8	8.9	57.4	19.2	22.7	28.4	27.0
18.9	33.3	10.0	16.8	22.3	25.3	77.6	35.3	44.4	13.2	57.4	29.5	57.7	69.0	70.7
4.7	3.5	13.0	12.7	10.4	15.4	13.6	5.1	6.5	1.5	8.4	8.2	6.9	8.0	7.9
391.8	260.6	207.8	111.6	296.1	162.4	143.1	404.2	114.2	99.0	278.8	107.4	173.2	204.4	88.2
0.4	0.7	2.1	1.8	3.5	3.7	2.8	6.9	3.3	2.1	29.4	2.0	2.4	2.4	2.4
5.2	6.4	39.7	25.7	56.9	53.5	24.8	39.8	22.8	6.1	49.5	15.1	14.1	14.7	14.8
1.2	0.4	0.1	0.1	0.1	0.7	1.6	4.7	5.6	0.9	0.3	0.3	4.1	6.7	6.7
78.1	9.5	24.7	10.2	11.8	44.7	87.0	131.2	77.8	16.1	7.9	28.3	75.3	35.3	30.5
108.0	14.8	35.6	31.0	53.9	132.5	380.9	444.2	393.8	40.2	11.0	67.4	287.0	146.1	144.9
28.0	100.4	30.4	11.1	32.0	51.3	21.7	19.7	44.7	221.4	48.5	10.3	211.5	37.9	45.6
20.9	7.0	43.4	99.4	56.9	54.2	53.1	43.1	22.7	5.5	37.5	41.1	25.0	24.3	24.5
29.0	24.3	7.0	4.1	6.4	4.4	94.9	94.1	75.3	29.7	18.6	9.4	16.3	37.4	41.5
61.3	40.9	326.1	248.5	272.7	331.6	296.2	881.9	260.3	45.6	531.5	284.9	151.7	154.0	162.0
14.7	8.4	26.4	36.1	54.6	23.3	32.8	33.2	29.4	16.8	88.0	31.7	20.5	21.7	22.7
34.2	16.2	56.6	86.5	125.3	48.9	67.5	72.8	63.1	35.3	187.2	77.4	46.2	47.4	49.4
4.5	2.2	7.0	11.4	16.3	5.6	7.4	8.6	7.1	4.0	21.2	10.2	5.8	5.6	6.1
17.1	8.4	26.4	46.7	64.3	20.3	26.0	31.6	24.6	13.7	73.8	39.2	22.3	20.2	21.9
4.1	1.9	6.3	12.3	14.2	5.8	6.6	7.9	5.8	2.6	12.8	9.5	4.9	4.5	4.9
0.7	0.5	1.3	2.1	2.2	1.0	1.3	1.1	0.8	0.3	1.6	1.5	0.9	0.9	0.9
4.3	1.9	7.1	14.5	14.1	7.0	8.0	9.7	5.6	2.2	12.3	9.9	5.2	4.9	5.3
0.7	0.3	1.4	2.8	2.3	1.7	1.7	1.9	1.1	0.3	1.8	1.8	1.0	0.9	0.9
4.6	1.8	9.4	19.1	13.5	12.5	11.8	12.4	6.6	1.7	10.0	11.4	5.8	5.8	5.9
0.9	0.4	2.1	4.3	2.7	3.0	2.7	2.6	1.3	0.3	1.9	2.3	1.2	1.1	1.2
2.6	1.1	6.4	13.6	7.8	9.7	8.6	7.6	3.9	0.9	5.4	6.5	3.4	3.2	3.5

(continued on next page)

Table 6 (continued)

	Sample no. 2-4	2-3	2-2	2-1	3A-5	3A-4	3A-3	3A-2	3A-1	3A-0	3B-1	3C-4	3C-3	3C-2	
t6.57															
t6.58	<i>in ppm</i>														
t6.59	Tm	0.3	0.5	0.4	0.7	0.5	1.9	1.2	0.7	1.7	2.0	0.8	0.2	0.4	0.3
t6.60	Yb	2.3	3.5	2.4	4.8	3.3	13.0	8.2	4.4	11.3	13.5	5.6	1.5	2.7	2.0
t6.61	Lu	0.3	0.5	0.3	0.7	0.5	1.9	1.2	0.7	1.6	2.0	0.9	0.2	0.4	0.3
t6.62	U/Th	0.43	1.94	0.49	0.30	9.76	4.58	1.23	2.17	19.24	1.49	7.07	1.55	2.69	3.88
t6.63	Sr/Ba	46.7	123.8	113.6	5.8	2.9	3.8	0.7	3.6	4.2	3.7	6.8	6.1	6.1	14.1

Ash: ashed at 750 °C; St: air dry base; SiO₂, Al₂O₃, K₂O, NaO, Fe₂O, and Ni are from XRF analysis, and all the others from ICP-MS. All data are whole coal-based.

mixed layers as have been identified by XRD. However, at least part of the MgO content is associated with carbonates, as indicated by the presence of dolomite in the XRD and SEM-EDX analyses (Table 5 and Figs. 6 and 7).

Fe is usually associated with pyrite in high sulphur coals, and a positive correlation between Fe and sulphur is commonly observed in most coal measures (Liu et al., 2001). However, this correlation has not been observed in the Heshan coals, and this is due to the strong organic affinity of sulphur, although significant amounts of pyrite in some samples were observed by optical microscopy and in the XRD and SEM-EDX analyses (Table 5 and Figs. 6 and 7). It is interesting that a significant positive correlation exists between Fe₂O₃ and P₂O₅, which suggests that at least part of the Fe is associated with phosphate minerals. The strengite (FePO₄·2H₂O) identified by the XRD analysis (Table 5 and Fig. 6) may well account for this association.

4.4. Trace element geochemistry

The trace element contents in the Heshan coals are summarised by seams in Table 6, and the mean values of these elements from Seams 3A, 3B, 3C, 4A, and 4B in the Suhe coal mine and their comparison with world averages and Chinese averages are given in Table 7. Compared to the world averages (Swaine, 1990), the Heshan coal is enriched with As, Be, Cd, Co, Cr, Cs, Ga, Mn, Mo, Nb, Rb, Sc, Sr, Ta, Th, Tl, U, V, W, Y, and Zr. Ta, U, W, and Mo are particularly enriched, having an enrichment factor (expressed as H/W in Table 7) of more than 15.0, more than 10 times the world averages. For all elements studied, only Ba, Bi, Cu, Ge, Ni, Pb, and Zn are relatively depleted. Of those elements with relatively high

levels, As, Be, Cd, Co, Cr, Mn, Mo, and U are on the US-EPA list of the most toxic elements (1990). If compared with some other Chinese coals (Ren et al., 1999), the elements Cd, Co, Cr, Mo, Pb, Rb, Sr, Th, U, and V have relatively high levels, with U showing the greatest enrichment (H/C = 6.42), whereas As, Ba, Cu, Mn, and Zn are relatively depleted.

In the Heshan coals, U has a maximum concentration of 175.8 ppm and Mo of 171.7 ppm (Tables 6 and 7). These relatively high values of the two elements occur in the top of Seam 4B (4B-7) and the lower part of Seam 3A (3A-1). The highest level of W (221.4 ppm) is recorded in the lower part of Seam 4B (4B-5). The abnormally high V values (>380 ppm) are recorded in the top of Seam 4B (4B-6, 4B-7) and the bottom of Seam 4A (4A-1). The highest value of Ta (29.4 ppm) occurs in the middle of Seam 4B (4B-4).

4.5. Trace element affinity and mode of occurrence

The ash content of coal is derived from three major sources: the inorganic matter associated with the original peat vegetation, the detrital and volcanoclastic input into the peat mire, and any epigenetic mineralisation. Each of these sources will have a characteristic trace element chemistry, so that correlations with ash content, particularly in the high-ash Heshan coals, where the detrital and volcanogenic contribution is large and variable, are difficult to interpret. In these circumstances, the diagnostic major elements are of much greater interpretative value for trace element affinity analysis than the ash percentage alone (Spears and Zheng, 1999). This is largely because the major elements can be shown to occur in particular, observable mineral phases within the coal, and thus a correlation between a trace and major element implies a specific mode of occurrence for the trace element.

3C-1	3C-0	4A-5	4A-4	4A-3	4A-2	4A-1	4B-7	4B-6	4B-5	4B-4	4B-3	4B-2	4B-1	4B-0
0.4	0.2	1.0	2.1	1.1	1.5	1.3	1.1	0.6	0.1	0.8	0.9	0.5	0.5	0.5
2.5	1.1	6.7	14.1	7.2	10.1	8.5	7.4	3.9	0.9	5.2	6.0	3.2	3.2	3.3
0.4	0.2	1.0	2.0	1.0	1.5	1.3	1.0	0.6	0.1	0.7	0.8	0.5	0.4	0.5
15.03	1.48	0.62	0.40	0.21	0.83	3.51	3.29	3.41	2.62	0.16	1.88	5.34	2.40	2.07
11.5	5.1	4.2	1.8	4.0	1.9	0.9	7.1	1.6	1.6	4.0	1.8	2.0	1.9	0.8

However, a negative correlation with the ash content suggests that an element is concentrated in the organic matter. For analysis of trace element affinity, several plots have been drawn based on the Pearson's correlation coefficients (r) between the elements.

In order to determine the predominant modes of occurrence for these trace elements, interplots have been further made between the correlation coefficients of these elements with different major elements, total sulphur, and ash. Fig. 8A is a plot of $r\text{Al}_2\text{O}_3$ against $r\text{Fe}$, from which three groups of elements can be distinguished. The first is the iron-related elements, including Zn, V, As, Tl, Ni, Cd, Cr, Rb, Cu, and Zr; the second is the aluminium-silicate-related elements, including Cs, Be, Th, Pb, Ga, and REE; and the third group is the aluminium-iron-silicate-related elements including Sc, Ge, and Bi. As indicated previously, Fe is positively correlated with P_2O_5 , which suggests that Fe is present in the form of iron-phosphate in addition to the more common sulphide association. Plots of $r\text{Fe}$ against $r\text{P}_2\text{O}_5$ can help to distinguish between sulphide and phosphate affinity of the Fe-related elements. Fig. 8B indicates a phosphate affinity for Zn, Rb, and Zr and suggests that all the other Fe-associated elements, including As, Cd, Cr, Cu, Ni, Tl, and V, may be present in iron-sulphide minerals. As noted above, iron carbonate has not been identified in these coals and the lack of correlation with Ca (Fig. 8C) confirms that these trace elements are unlikely to have a carbonate association. This analysis suggests that Zn may be associated with iron-phosphate minerals, which contrasts with the observations of Palmer and Lyons (1996) and Spears and Zheng (1999) who concluded that Zn is mainly associated with carbonate minerals.

Sr and Mn show a positive correlation with both CaO and the ash contents, indicating a carbonate

affinity (Fig. 8C). W has a positive correlation with CaO ($r=0.41$) but a less significant correlation with the ash content ($r=0.12$), which may imply a mixed carbonate and organic affinity. Finkelman (1981) found that W was largely organically associated in US coals, although Rose (2001) demonstrated a mixed carbonate/sulphide and silicate mode of occurrence in UK anthracites. Palmer and Lyons (1996) noted that calcite, where present, is a major contribution of Sr and also Zn and Ni.

U and Mo are solely associated with the total sulphur and significant inverse correlation with ash contents. Therefore, they are inferred to have an organic affinity.

Ba shows very weak correlation with total sulphur ($r=0.24$), and this may suggest a possible barium-sulphate affinity.

Ta shows positive correlations with the ash yields ($r=0.36$) and with MgO ($r=0.54$), indicating a magnesium-containing mineral association. It is unlikely that this is a carbonate as Ta shows no correlation with either CaO or Fe. A slight correlation with Al_2O_3 ($r=0.3$) suggests a Mg-bearing clay mineral as a possible candidate.

Y shows less significant correlation with Al_2O_3 ($r=0.23$) and significant correlation with the REE ($r=0.66$), implying an overall clay mineral association.

The modes of occurrence of Co and Nb are more difficult to infer from the present data. The Co shows a weak correlation with ash contents ($r=0.17$) but has fair to significant relationships with Fe ($r=0.3$), Bi ($r=0.38$), and W ($r=0.52$), which might suggest a mixed sulphide and organic mode of occurrence as was inferred for Co in UK anthracites by Rose (2001). Nb also shows a weak correlation with the ash contents ($r=0.12$) but has significant relationships with MgO ($r=0.34$), TiO_2 ($r=0.54$), Cs ($r=0.43$),

Table 7

Mean values of major and trace elements from Heshan coals in the Suhe coal mine and their comparison with world and Chinese averages

	Heshan coals				Chinese coal range (Ren et al., 1999)				Swaine's worldwide ranges (Querol et al., 1999)			
	Min.	Max.	Mean	S.D.	Min.	Max.	Mean	H/C	Min	Max	Mean	H/W
Ash (%)	13.18	91.17	58.19	20.25								
St (%)	0.37	11.58	5.87	3.12								
<i>in wt.%</i>												
SiO ₂	7.26	42.06	24.85	7.90								
Al ₂ O ₃	2.58	16.23	7.45	4.21								
CaO	0.02	24.79	2.28	5.54								
MgO	0.09	1.11	0.44	0.23								
K ₂ O	0.11	1.57	0.69	0.34								
Na ₂ O	0.00	0.48	0.10	0.15								
Fe ₂ O ₃	0.00	4.60	1.58	1.18								
TiO ₂	0.00	0.58	0.21	0.14								
P ₂ O ₅	0.00	0.02	0.01	0.01								
<i>in ppm</i>												
As	2.1	70.1	19.2	20.0	0.21	32,000	276.61	0.07	0.5	80	29	1.92
Ba	27.4	321.9	79.2	56.6	4.1	1540	169.01	0.47	20	1000	120	0.40
Be	0.3	6.5	2.4	1.5					0.1	15	3	1.21
Bi	0.1	2.6	0.7	0.5					2	20		0.13
Cd	0.0	3.2	0.5	0.6	0.04	1.2	0.46	1.12	0.1	3	0.5	1.03
Co	3.4	23.0	10.2	5.0	0.03	39.6	6.72	1.51	0.5	30	4	2.03
Cr	5.3	321.3	76.2	90.7	0.46	942.7	34.87	2.19	0.5	60	8	3.81
Cs	0.5	18.0	6.3	4.4					0.3	5		3.59
Cu	4.3	30.2	12.6	6.4	4.28	133.7	28.22	0.45	0.5	50	7	0.84
Ga	3.4	33.9	14.6	9.0					1	20	2.3	1.69
Ge	0.2	1.7	0.6	0.4					0.5	50	7	0.12
Mn	4.0	270.9	82.0	71.0	6.02	8540	271.22	0.30	5	300	70	1.17
Mo	2.5	171.7	45.6	49.9	0.2	241	18.15	2.51	0.1	10	4	15.20
Nb	2.8	119.2	23.3	27.8					1	20		5.96
Ni	0.0	27.0	6.9	2.0	1.1	255	22.62	0.30	0.5	50	13	0.34
Pb	8.9	135.3	29.7	25.1	5.28	69.7	24.77	1.20	2	80	59	0.74
Rb	5.4	84.8	38.2	21.8	1.4	408	20.68	1.85	2	50	15	2.55
Sc	1.5	17.5	8.1	3.8					1	10	4	1.54
Sr	88.2	3388.7	551.8	840.5	4.9	894	175.96	3.14	15	500	240	2.76
Ta	0.4	29.4	2.9	5.3					0.1	1		29.42
Th	3.6	58.5	22.5	16.9	0.09	25.4	6.9	3.25	0.5	10	4	5.61
Tl	0.1	6.7	1.7	2.0					<0.2	1		6.72
U	6.9	175.8	48.3	45.0	0.16	199.3	7.52	6.42	0.5	10	2	24.14
V	11.0	444.2	138.3	123.2	3.4	1292	94.11	1.47	2	100	19	3.46
W	10.3	221.4	58.0	51.4					0.5	5		44.28
Y	5.5	99.4	37.4	26.1					2	50		1.99
Zn	4.1	98.5	40.5	27.8	0.56	193	43.24	0.94	5	300	20	0.81
Zr	40.9	881.9	246.7	224.9					5	200	28	4.41
La	5.0	88.0	28.2	17.1								
Ce	12.0	187.2	63.2	37.4								
Pr	1.6	21.2	7.7	4.5								
Nd	6.0	73.8	29.3	17.4								
Sm	1.5	17.4	7.0	4.0								
Eu	0.3	2.5	1.1	0.5								
Gd	1.5	19.8	7.6	4.5								
Tb	0.3	3.3	1.4	0.8								
Dy	1.7	20.2	8.8	5.4								

Table 7 (continued)

	Heshan coals				Chinese coal range (Ren et al., 1999)				Swaine's worldwide ranges (Querol et al., 1999)			
	Min.	Max.	Mean	S.D.	Min.	Max.	Mean	H/C	Min	Max	Mean	H/W
t7.60	<i>in ppm</i>											
t7.61	Ho	0.3	4.3	1.9	1.2							
t7.62	Er	0.9	13.6	5.5	3.7							
t7.63	Tm	0.1	2.1	0.8	0.6							
t7.64	Yb	0.9	14.1	5.6	3.8							
t7.65	Lu	0.1	2.0	0.8	0.6							
t7.66	Th/U	0.1	6.2	0.9	0.3							
t7.67	Sr/Ba	0.7	14.1	4.1	0.6							

H/C=ratio of concentrations in mean Heshan coal and mean Chinese coal; H/W=ratio of mean concentrations in Heshan coal and mean worldwide coal.

Ta ($r=0.8$), Th ($r=0.48$), and Zn ($r=0.66$), which again may imply a mixed mode of occurrence, partly organic and partly clay mineral association.

Of the rare earth elements (REE), Th has positive correlation with Al_2O_3 ($r=0.67$), suggesting that it is mainly associated with clay minerals. La, Ce, Pr, Nd, and Eu have slightly positive correlations with the Al_2O_3 ($r>0.34$) and thus may have a partial clay mineral association, being adsorbed on the clays. The remaining REE (Sm, Gd, Tb, Dy, Ho, Er, Tm, Yb, and Lu) show no clear relationships with other components and their mode of occurrence is problematical.

5. Depositional environment of the Heshan coals

Previous studies have suggested that the Heshan coals accumulated in mires developed on tidal flats associated with isolated carbonate platforms, surrounded by deeper water facies (Shao et al., 1998, 2003). The coal-forming materials are believed to be mangrove-like plants which can grow in an alkaline, brackish, and saline environment (Shao et al., 1998). This represents an unusual coal-forming environment, contrasting with the more common siliciclastic association of coal measures. All the evidence, such as the abnormally high organic sulphur, the presence of marine fossils in the coals and the interclays, and the presence of some authigenic minerals including dolomite and calcite, indicate an alkaline environment for peat accumulation. In addition to these, the sulphur contents, petrographical data, and major and trace elements of the coal may provide further support for this hypothesis.

The sulphur in marine-influenced coal is largely controlled by availability of the marine sulphate, so that the extent of marine influence is reflected in the concentration of sulphur in the coal (Casagrande et al., 1977; Chou, 1990; Spears et al., 1999; Gayer et al., 1999). Particularly, the organic sulphur may be closely related to the original salinity of the groundwater in the palaeomire. The Heshan coals have not only a marine roof but also a marine limestone floor, and the sulphur concentration in the coals is much higher than in most coals from siliciclastic coal measures. This strongly suggests that these coals formed in a more fully marine environment. The organic sulphur in low sulphur coals is believed to originate from plants (Smith and Batts, 1974; Price and Shieh, 1979; Casagrande, 1987). Nevertheless, the abnormally high organic sulphur contents in the Heshan coals cannot be accounted for by the original plant sulphur alone. Present-day marine mangrove peats from the Little Shark area of the Florida Everglades have only 2–4% of organic sulphur (Casagrande et al., 1977). Therefore, there must have been another source of sulphur which combined into the peat after the plants died and were buried. We believe that the high organic sulphur in the Heshan coals could be more reasonably explained as a result of bacterial reduction of marine sulphate and subsequent incorporation of reduced sulphur into the organic matrix. The relatively low pyrite content of the Heshan coals is due to the minimal input of terrestrial iron by freshwater, which is consistent with the carbonate platform setting in central Guangxi, remote from any terrestrial input.

It should be noted that many coals in which no significant marine influence can be detected have

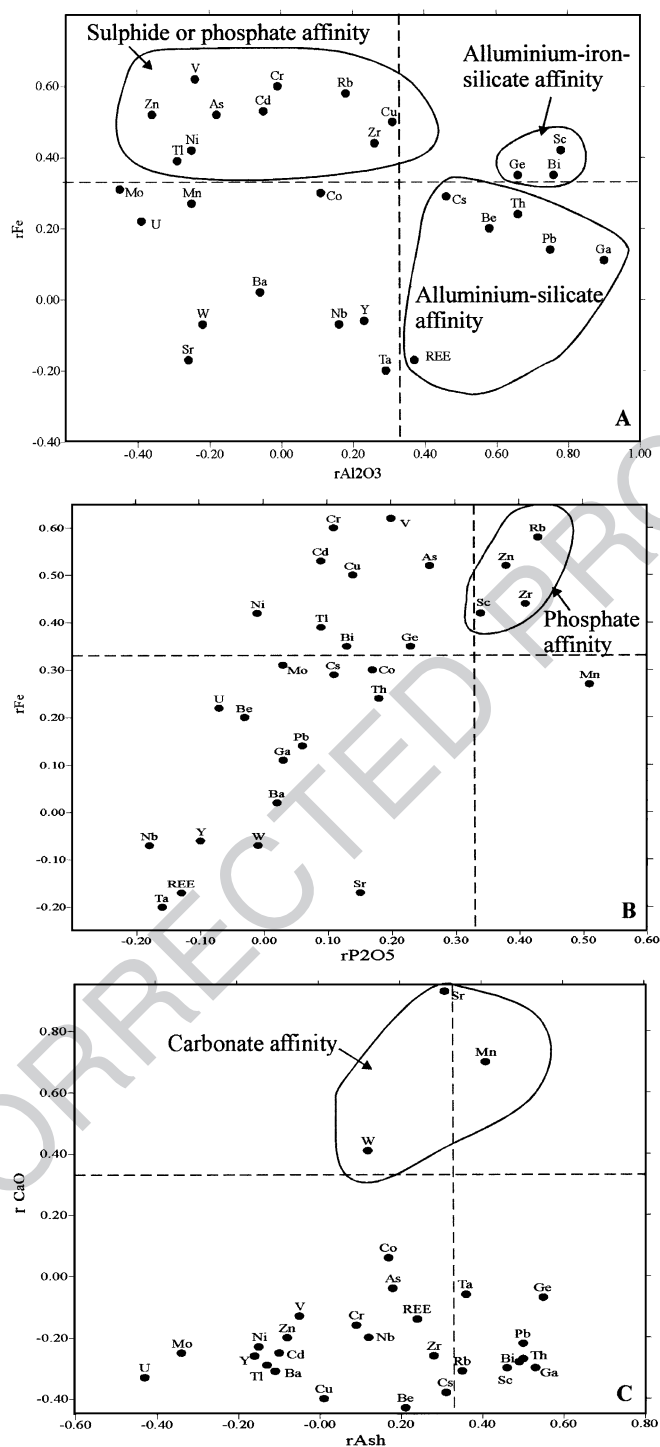


Fig. 8. Cross-plots of the Pearson's correlation coefficients (r) for major and trace elements with respect to contents of total iron, Al_2O_3 , P_2O_5 , CaO and ash. (A) Plot of $r_{Fe}-r_{Al_2O_3}$; (B) plot of $r_{Fe}-r_{P_2O_5}$; (C) $r_{CaO}-r_{Ash}$. Dashed lines represent $r=0.33$ indicating a 95% confidence level for correlation. Areas indicating likely mineral affinities are outlined, see text for discussion.

high concentrations of sulphur, e.g. many of the Tertiary coals of the circum-Mediterranean basins (Querol et al., 1996; Karayigit et al., 2000, 2001) and the Tertiary coals of intracontinental rift basins of Europe (Bouška et al., 1997). The sulphur in these coals is commonly derived from sulphide- and sulphate-rich rocks in the source land of the basins, as has been demonstrated by sulphur isotope studies (e.g. Bouška et al., 1997). In these basins, also, U, Mo, and W have a major organic affinity (Querol et al., 1996).

The relatively high GI values and very low TPI values indicate that the Heshan coal might have formed in an environment with a generally high water table and high pH values. Strongly alkaline conditions would have favoured the bacterial breakdown of the plant tissue in the peat. Vertical distributions of macerals through the Heshan coals (Fig. 5) show episodic changes with corresponding high and low values of different indices including GI, TPI, and vitrinite–intertinite ratio. Seam 4B has relatively high GI and low TPI, implying a palaeomire with a higher water table and higher pH value. Compared with Seam 4B, Seam 4A has relatively low GI and high TPI, indicating a lower water table and lower pH values for the palaeomire. The amalgamated Seam 4 in the Lilan coal mine is about 1.80 m thick and shows an upward decreasing GI and increasing TPI, which is consistent with the overall maceral compositions of Seams 4A and 4B. Seams 3A, 3B, and 3C have comparatively higher values of GI and lower TPI, compared with Seam 4A, implying that these seams might have formed in mires with a higher water table and higher pH values. A more complete analysis of the relationship between coal-forming mire development and sea-level variations, and its sequence stratigraphic significance, has been documented by Shao et al. (2003).

The geochemical data also show some vertical variations within the seams (Fig. 9), reflecting overall trends of marine influence in the palaeomires. The very high contents of total sulphur (5.3–11.6%), CaO (0.22–37.12%), and Sr (107–3389 ppm) are the result of a strong marine influence. The overall high values of the total sulphur in Seams 3A, 3B, and 3C imply a stronger influence from marine water in these seams. It is interesting that the CaO and Sr show upward increasing trends in Seams 4B and 4A, which may imply that the marine influence was becoming

stronger towards the top of the palaeomires. Similarly, upward decreasing trends in Sr and CaO in Seam 3A may indicate a lessening marine influence. It is also noticeable that Seam 4A has much higher aluminium contents than in other seams, which may suggest a greater influx of weathering products in the palaeomire of this seam during deposition.

Very high uranium contents have been found in the Heshan coals. The enrichment of U in coals has been attributed to the episodic inundation of the coal depositional environment by marine waters (Van der Flier and Fyfe, 1985). This is due to seawater being relatively enriched in soluble oxidised U complexes, such as UO_2^{2+} , which are reduced by humic acids in the peat mire to less soluble uranous forms. These can form complexes with organic matter or be adsorbed onto clay minerals. In the Heshan coals, the positive correlation between total (mainly organic) sulphur and U contents indicates the affinity of the uranium to organic matter. This is in good agreement with the inferred depositional environments for the Heshan coals (Shao et al., 1998). The actinide elements Th and U can be used for palaeoenvironmental interpretation (Van der Flier and Fyfe, 1985), and the Th/U ratios within the Heshan coals may provide further evidence of marine influence in these coals. Plots of Th/U ratios against depth are given in Fig. 9. Taylor and McLennan (1985) gave an average Th/U ratio for Post-Archean shales of 4.8–0.3 and suggested that ratios >4.8 indicate relative enrichment of Th, and ratios <4.8 indicate relative enrichment of U. In the Heshan coals, Th/U ratios vary between 0.05 and 6.22, with an average of 0.29. The lowest Th/U ratios occur in Seams 3A, 3B, and 3C (Fig. 9), which may suggest a stronger marine influence in these seams than in Seams 2, 4A, and 4B. In Seams 3A and 3C, the lowest Th/U ratios occur in the basal coal layer in each seam, which implies a decreasing marine influence upwards through the seams, in agreement with the Ca and Sr data. However, caution should be exercised in relying too heavily on U enrichment as an indicator of marine influence. U enrichment has been noted in coals that demonstrably had no marine influence, e.g. the Oligocene coals of the Mequinenza Formation in the South Pyrenean Ebro foreland basin (Querol et al., 1996). Here, it has been argued that strongly alkaline conditions, resulting from the recycling of sulphate and carbonate lithologies in earlier

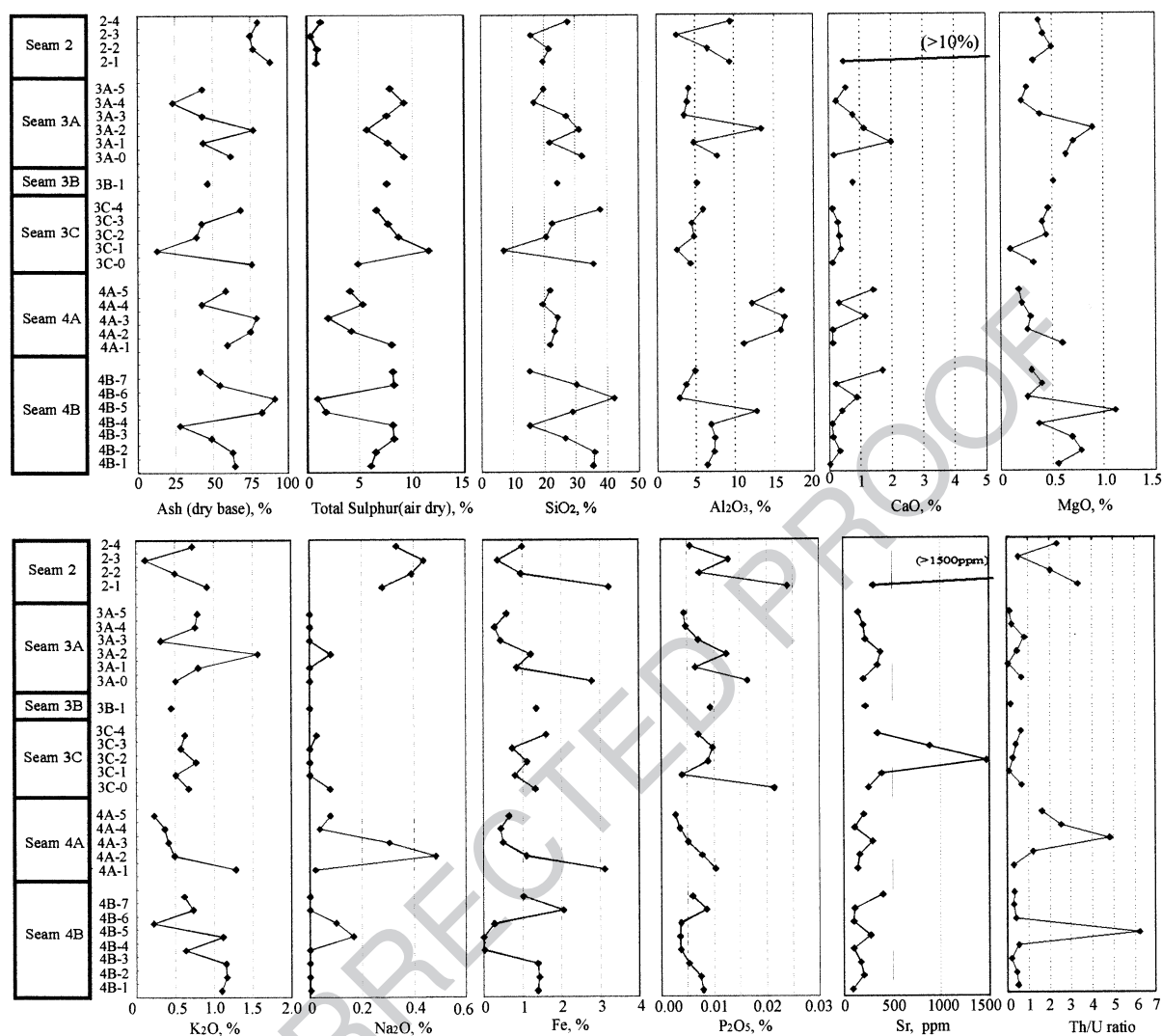


Fig. 9. Vertical trends of total sulphur contents, ash yields and some major and trace elements in Seams 3A, 3B, 3C, 4A and 4B in the Suhe coal mine, Heshan Coalfield, central Guangxi. No vertical scale is intended—see Fig. 5 for the seam thicknesses.

deposits of the basin, were responsible for U enrichment in the groundwater of the peat mire (Querol et al., 1996). U enrichment is thus likely an indicator of alkaline groundwater conditions, which, in the case of the Heshan Formation coals, were produced by marine transgression.

In spite of the above evidence suggesting a major marine influence during the deposition of the Heshan coals, the presence of iron-phosphate minerals implies a freshwater influence during palaeomire development. It has been documented that the concentration

of total iron in freshwater is 197 times higher than in seawater (Diessel, 1992), suggesting that the majority of iron is ultimately sourced from the land. Strengite ($\text{FePO}_4 \cdot 2\text{H}_2\text{O}$) is found to be the major iron-phosphate mineral in the Heshan coals which is usually enriched in the lower half of each seam. The iron-phosphate is believed to be derived mainly from freshwater (Nelson, 1967). It is also noticeable that Fe and P_2O_5 have a close relationship and both are present at higher levels at the base of most of the Heshan coals. This may result from the development

of palaeosols near the base of the coal seams. In particular, the base of Seam 4A is an obvious discontinuity surface (Shao and Zhang, 1992). The upward decreasing trends of both Fe and P_2O_5 within Seam 4A, 3C, and 2 (Fig. 9) indicate that the freshwater had a stronger influence during the early stages of the palaeomire development. The low levels of Fe in the higher parts of these seams may reflect the low levels of Fe in the groundwater over these carbonate platforms, remote from a terrigenous detrital source. This result would appear to contradict the Th/U ratio pattern in Seam 3C, discussed above, where the lowest Th/U ratio occurs in the basal coal layer (sample 3C-1). However, the basal layer of Seam 3C (sample 3C-0), in which the high levels of Fe and P_2O_5 occur, lies beneath the lowest coal layer, suggesting a rapid transition from freshwater in the chert to marine water in the overlying coal.

From above analysis, we believe that the Heshan coals were formed in mires with a relatively high concentration of saline water. The high ash contents imply low-lying mires, with an influx of detrital material and dissolved ions. The low TPI values reflect strong microbial activity in association with a high water table. Geochemical parameters suggest that marine influence increased throughout the peat mire development. The lithofacies of the roof and base of the coal seams are mainly tidal-flat facies with laminated clayey algal-clast packstones, suggesting that the coal-forming mires were developed on a tidal-flat environment. Thus, this study confirms that the coal-forming materials were most likely derived from mangrove-like plants that tolerated variable mixtures of alkaline, brackish to fully marine seawater in tide-influenced swamps, which were similar to modern intertidal mangrove swamps (Shao et al., 1998).

6. Conclusions

(1) The sulphur contents in the Heshan coals (with ash less than 50%) range from 5.3% to 11.6%, of which 92% is organic sulphur. The SEM-EDX analysis shows that the average organic sulphur content of the vitrinite group macerals is 8.3%, which is higher than that in the inertinite group macerals, with an average of 7.08%. The high

vitrinite reflectance (1.8–2.04% $R_{o,m}$) indicates that the Heshan coals in the Heshan Coalfield are mainly low-volatile bituminous coal.

- (2) The coal is composed of vitrinite and inertinite macerals with low TPI and high GI values, suggesting a unique palaeoenvironment with alkaline, high-pH water conditions. This may represent the characteristics of a low-lying mire developed in a marine carbonate platform setting.
- (3) The minerals in the Heshan coals are mainly quartz, calcite, dolomite, kaolinite, illite, and pyrite. The minor minerals in the coals are marcasite, strengite, and feldspar, as well as some weathering oxidation products such as gypsum.
- (4) Major elements in the Heshan coals have higher concentrations compared to the coals in non-marine siliciclastic coal measures, which is consistent with the high ash yields of the Heshan coals. In particular, very high levels of SiO_2 reflect the predominance of quartz, and high levels of CaO are consistent with the presence of calcite and dolomite in the coals.
- (5) Most trace elements in the Heshan coals are enriched with respect to their world ranges, in particular, Mo, Ta, U, and W are highly enriched, being more than 10 times their world means. These trace elements are believed to be associated either with minerals or organic matter. The mineral associations include aluminium-silicates (such as Cs, Be, Th, Pb, Ga, and REE), aluminium-iron-silicates (such as Sc, Ge, and Bi), iron-phosphates (Zn, Rb, and Zr), iron-sulphides (such as As, Cd, Cr, Cu, Ni, Tl, and V), carbonates (Sr, Mn, and W), and possibly barium-sulphate (Ba). U and Mo are associated with the organic matter.
- (6) The coal-forming environments for the Heshan coals are believed to be low-lying, marine-influenced palaeomires developed on carbonate platforms. This can be demonstrated by the abnormally high organic sulphur contents, high ash yields, relatively high GI values, very low TPI values, very high U contents, and very low Th/U ratios, as well as the presence of a marine limestone in the roof and floor of the coal seams. Seams 3A, 3B, and 3C may have experienced a stronger marine influence than Seams 2, 4A, and 4B.

(7) The Heshan coals have several features in common with coals from the Tertiary circum-Mediterranean coal basins, despite the complete absence of marine influence in the latter. The similarities include the following: high contents of organic sulphur; enrichment in U, Mo, and W; the predominant organic affinity of U; relatively high values of GI; and relatively low contents of Fe. It is considered that these similarities were produced by a common strongly alkaline ground-water chemistry, unusual in most coal-forming mires.

Acknowledgements

This research was supported by a research fellowship to LS from the Cardiff University China Center, the State Natural Science Foundation of China (NSFC) (Award No. 40172050 and No. 49772129), and the Excellent Young Teachers Program (EYTP) of Ministry of Education of China. We thank Peter Fisher, Sarah Goldsmith, Colin Lewis and Tony Oldroyd for technical assistance with the SEM, ICP-MS, XRF, and XRD analyses, respectively. The text has been greatly improved as a result of insightful comments from an anonymous reviewer.

References

Beijing Coal Chemistry Institute, 1982. Handbook for Coal Analyses, 2nd ed. Coal Industry Publishing House, Beijing, pp. 89–105. In Chinese.

Bouška, V., Pešek, J., Zák, K., 1997. Values of $\delta^{34}\text{S}$ in iron disulphides of the northern Bohemian Lignite Basin, Czech Republic. In: Gayer, R.A., Pešek, J. (Eds.), *European Coal Geology and Technology*. Geological Society Special Publications, vol. 125, pp. 261–267.

Casagrande, D.J., 1987. Sulphur in peat and coal. In: Scott, A.C. (Ed.), *Coal and Coal-Bearing Strata: Recent Advances*. Geological Society Special Publications, vol. 32, pp. 87–105.

Casagrande, D.J., Siefert, K., Berschinski, C., Sutton, N., 1977. Sulphur in peat-forming systems of Okefenokee swamp and Florida everglades: origin of sulphur in coal. *Geochimica et Cosmochimica Acta* 41, 161–167.

Chen, J., 1987. A further study on the coalification model of the Upper Permian carbonate coal measures in southern China. *Proceedings of the Symposium on China's Permo-Carboniferous Coal-Bearing Strata and Geology*. Science Press, Beijing, China, pp. 217–223.

Chou, C.-L., 1990. Geochemistry of sulphur in coal. In: Orr, W.L., White, C.M. (Eds.), *Geochemistry of Sulphur in Fossil Fuels*. American Chemical Society Symposium Series 429, pp. 30–52. Chapter 2.

China National Administration of Coal Geology (CNACG), 1996. *Sedimentary Environments and Coal Accumulation of Late Permian Coal Formations in Western Guizhou, Southern Sichuan and Eastern Yunnan*. Chongqing University Press. 277 pp., in Chinese.

Diessel, C.F.K., 1982. An appraisal of coal facies based on maceral characteristics. In: Mallett, C.W. (Ed.), *Coal Resources—Origin, Exploration and Utilization in Australia*. Australian Coal Geology, vol. 4, pp. 474–484.

Diessel, C.F.K., 1986. On the correlation between coal facies and depositional environments. *Advances in the Study of the Sydney Basin. Proceedings of 20th Symposium of University of Newcastle*, pp. 19–22.

Diessel, C.F.K., 1992. *Coal-Bearing Depositional Systems*. Springer-Verlag, Berlin. 721 pp.

Feng, Z., Jin, Z., Yang, Y., Bao, Z., Xin, W., 1995. *Lithofacies Palaeogeography of Permian of Yunnan–Guizhou–Guangxi Region*. Geological Publishing House, Beijing. 146 pp.

Finkelman, R.B., 1981. Modes of occurrence of trace elements in coals. *US Geol. Surv. Open-file Rep.*, No OFR-81-99. 301 pp.

Finkelman, R.B., Gross, P.M.K., 1999. The types of data needed for assessing the environmental and human health impacts of coal. *International Journal of Coal Geology* 40, 91–101.

Gayer, R.A., Rose, M., Dehmer, J., Shao, L.-Y., 1999. Impact of sulphur and trace element geochemistry on the utilization of a marine-influenced coal: case study from the South Wales Variscan foreland basin. *International Journal of Coal Geology* 40, 151–174.

Gentzis, T., Goodarzi, F., 1990. Petrology, depositional environment and utilization potential of Late Paleocene coals from the Obed–Marsh deposit, West-Central Alberta, Canada. *International Journal of Coal Geology* 16, 287–308.

Han, D., Yang, Q., 1980. *Coalfield Geology of China*, vol. II. China Coal Industry Press. 415 pp., in Chinese.

Hou, X., Ren, D., Mao, H., Lei, J., Jin, K., Chu, P.K., Reich, F., Wayne, D.H., 1995. Application of imaging TOF-SIMS to the study of some coal macerals. *International Journal of Coal Geology* 27, 23–32.

Hu, S., 1994. On the event Dongwu movement and its relation with Permian subdivision. *Journal of Stratigraphy* 18 (4), 309–315 (in Chinese with English abstract).

Huang, N., Wen, X., Huang, F., Wang, G., Tao, J., 1994. The Paleosol bed and the coal deposition model in Heshan coal field, Guangxi, China. *Acta Sedimentologica Sinica* 12 (1), 40–46 (in Chinese with English abstract).

Jin, H., Li, J., 1987. The depositional environment of the Late Permian in the Matan area, Heshan county, Guangxi Province. *Scientia Geologica Sinica* 20 (1), 61–69 (in Chinese with English abstract).

Karayigit, A.I., Spears, D.A., Booyh, C.A., 2000. Distribution of environmental sensitive trace elements in the Eocene Sorgun coals, Turkey. *International Journal of Coal Geology* 42 (4), 297–314.

- 960 Karayigit, A.I., Gayer, R.A., Ortac, F.E., Goldsmith, S., 2001.
961 Trace elements in the Lower Pliocene fossiliferous Kangal lig-
962 nites, Sivas, Turkey. *International Journal of Coal Geology* 47,
963 73–89.
- 964 Liao, Z., 1980. Upper Permian brachiopods from western Guizhou.
965 Stratigraphy and Palaeontology of Upper Permian Coal-Bearing
966 Formations in Western Guizhou and Eastern Yunnan, China.
967 Nanking Institute of Geology and Palaeontology, Academia Sin-
968 ica, Nanjing, China Science Press, Beijing, pp. 241–277.
- 969 Liu, B., Xu, X., Pan, X., Huang, H., Xu, Q., 1993. Sedimentary
970 Crust Evolution and Mineral Formation of South China. Science
971 Press, Beijing. 236 pp., in Chinese.
- 972 Liu, D., Yang, Q., Tang, D., Kang, X., Huang, W., 2001. Geo-
973 chemistry of sulfur and elements in coals from the Antaibao
974 surface mine, Pingshuo, Shanxi Province, China. *International*
975 *Journal of Coal Geology* 46, 51–64.
- 976 Mei, S., Zhu, Z., Shi, X., Sun, K., Li, B., 1999. Sequence stratig-
977 raphy of Permian Lopingian strata in central Guangxi. Geo-
978 sciences—Journal of Graduate School, China University of
979 Geosciences 13 (1), 11–18 (in Chinese with English abstract).
- 980 Nelson, B.W., 1967. Sedimentary phosphate method for estimating
981 paleosalinities. *Science* 158, 917–920.
- 982 Nicholls, G.D., 1968. The geochemistry of coal-bearing strata. In:
983 Murchison, D., Westoll, T.S. (Eds.), *Coal and Coal Bearing*
984 *Strata*. Oliver & Boyd, Edinburgh. 418 pp.
- 985 Palmer, C.A., Lyons, P.C., 1996. Selected elements in major min-
986 erals from bituminous coal as determined by INAA: implica-
987 tions for removing environmentally sensitive elements from
988 coal. *International Journal of Coal Geology* 32, 151–166.
- 989 Price, F.T., Shieh, Y.N., 1979. The distribution and isotopic com-
990 position of sulphur in coals from the Illinois basin. *Bulletin of*
991 *the Society of Economic Geologists* 74, 1445–1461.
- 992 Querol, X., Cabrera, L., Pickel, W., Lopez-Soler, A., Hagemann,
993 H.W., Fernandez-Turiel, J.L., 1996. Geological controls on the
994 coal quality of the Mequinenza subbituminous coal deposit,
995 northeast Spain. *International Journal of Coal Geology* 29,
996 67–91.
- 997 Querol, X., Finkelman, R.B., Alastuey, A., Huerta, A., Palmer,
998 C.A., Mroczkowski, S., Kolker, A., Chenery, S.N.R., Robin-
999 son, J.J., Lopez-Soler, A., 1998. Quantitative determination of
1000 modes of occurrence of major, minor and trace elements in
1001 coal: a comparison of results from different methods. *Proceed-*
1002 *ings of the AIE 8th Australian Coal Conference*, December
1003 1998, pp. 51–56.
- 1004 Querol, X., Alastuey, A., Plana, F., Lopez-Soler, A., Tuncali, E.,
1005 Toprak, S., Ocakoglu, F., Kolker, A., 1999. Coal geology and
1006 coal quality of the Miocene Mugla basin, southwestern Anato-
1007 lia, Turkey. *International Journal of Coal Geology* 41, 311–332.
- 1008 Ren, D., Zhao, F., Wang, Y., Yang, S., 1999. Distributions of minor
1009 and trace elements in Chinese coals. *International Journal of*
1010 *Coal Geology* 40, 109–118.
- 1011 Rose, M., 2001. Aspects of the inorganic trace element geochem-
1012 istry and associated mineralogy in coals from South Wales.
1013 Unpublished PhD thesis, University of Wales. 248 pp.
- 1014 Sha, Q., Wu, W., Fu, J., 1990. Synthetic Studies on Permian Series
1015 in Guizhou and Guangxi. Science Press, Beijing, China. 215 pp.,
1016 in Chinese.
- Shao, L., Zhang, P., 1992. Disconformities and cycles of Upper
Permian in central Guangxi, southern China. *Journal of China*
Coal Society 17, 19–26 (in Chinese with English abstract).
- Shao, L., Zhang, P., 1999. Late Permian submarine fan turbidite
facies in the Laibin–Heshan area of Guangxi. *Journal of Palae-*
ogeography 1 (1), 20–31 (in Chinese with English abstract).
- Shao, L., Zhang, P., Shen, S., Lei, J., Dou, J., Fan, B., 1995.
Sedimentology and sequence stratigraphy of Late Permian
coal-bearing carbonate successions in Guizhou and Guangxi,
southern China. Unpublished internal report of the project of
the coal science foundation of China and the State Natural
Science Foundation of China, Beijing Graduate School of
China University of Mining and Technology. 102 pp. (in Chi-
nese).
- Shao, L., Zhang, P., Ren, D., Lei, J., 1998. The Late Permian coal-
bearing carbonate sequences in South China: coal accumulation
on carbonate platforms. *International Journal of Coal Geology*
37, 235–257.
- Shao, L., Zhang, P., Gayer, R.A., Chen, J., Dai, S., 2003. Coal in a
carbonate sequence stratigraphic framework: the Upper Permian
Heshan Formation in central Guangxi, southern China. *Journal*
of the Geological Society, London 160, 1–15.
- Shen, S., Fan, B., Shao, L., Fu, S., 1995. Study of biostratigraphic
correlation of the Late Permian coal seams in Guizhou and
Guangxi Provinces. *Coal Geology and Exploration* 23 (6), 1–5
(in Chinese).
- Sheng, J.Z., Jin, Y.G., 1994. Correlation of Permian deposits in Chi-
na. *Palaeoworld* 4 Nanjing Univ. Press, Nanjing, pp. 14–113.
- Smith, J.W., Batts, B.D., 1974. The distribution and isotopic com-
position of sulphur in coal. *Geochimica et Cosmochimica Acta*
38, 121–133.
- Spears, D.A., Zheng, Y., 1999. Geochemistry and origin of ele-
ments in some UK coals. *International Journal of Coal Geology*
38, 161–179.
- Spears, D.A., Manzanares-Papayanopoulos, L.I., Booth, C.A.,
1999. The distribution and origin of elements in a UK coal:
the importance of pyrite. *Fuel* 78, 1671–1677.
- Stach, E., Mackowsky, M.-T., Teichmüller, M., Taylor, G.H., Chan-
dra, D., Techmüller, R., 1982. *Stach's Textbook of Coal Petrol-*
ogy, 3rd ed. Borntraeger, Stuttgart. 535 pp.
- Swaine, D.J., 1990. *Trace Elements in Coal*. Butterworth, London.
278 pp.
- Taylor, S.R., McLennan, S.M., 1985. *The Continental Crust: Its*
Composition and Evolution. Blackwell, Oxford. 312 pp.
- Van der Flier, E., Fyfe, W.S., 1985. Uranium–thorium systematics
of two Canadian coals. *International Journal of Coal Geology* 4,
335–353.
- Wang, Y., Jin, Y., 2000. Permian palaeogeographic evolution of the
Jiangnan Basin, South China. *Palaeogeography, Palaeoclimatol-*
ogy, *Palaeoecology* 160, 35–44.
- Wang, L., Lu, Y., 1994. *The Permian Lithofacies Paleogeography*
and *Mineral Deposits in South China*. Geological Publishing
House, Beijing, China. 147 pp., in Chinese.
- Zhang, P., Shao, L., 1987. A study on organic reefs from the Late
Permian Heshan Formation in the Etan–Matan area, central
Guangxi, South China. *Proceedings of the Symposium on Chi-*
na's Permo-Carboniferous Coal-Bearing Strata and Geology.

1074 Science Press, Beijing, China, pp. 332–340. In Chinese with
1075 English abstract.
1076 Zhang, P., Liu, H., Zhuo, Y., Jia, Y., Yin, Z., 1983. On restricted
1077 platform carbonate coal Formation: some sedimentary character-
1078 istics of Heshan Formation in the Heshan area of central Guangxi.
1079 *Acta Sedimentologica Sinica* 1 (3), 16–28 (in Chinese with
1080 English abstract).

Zhuang, X., Querol, X., Zeng, R., Xu, W., Alastuey, A., Lopez-
Soler, A., Plana, F., 2000. Mineralogy and geochemistry of coal
from the Liupanshui mining district, Guizhou, South China.
International Journal of Coal Geology 45, 21–37.

1081
1082
1083
1084